Two-flavor Color Superconductivity in Magnetic Field

by

Lang Yu

A Dissertation Presented in Partial Fulfillment
of the Requirements for the Degree
Doctor of Philosophy

Approved April 2012 by the
Graduate Supervisory Committee:

Igor Shovkovy, Chair
Cecilia Lunardini
Kevin Schmidt
Ricardo Alarcon
Richard Lebed

ARIZONA STATE UNIVERSITY

May 2012

ABSTRACT

Quark matter at sufficiently high density and low temperature is expected to be a color superconductor, and may exist in the interior of neutron stars. The properties of two simplest possible color-superconducting phases, i.e., the color-flavor locked (CFL) and two-flavor superconducting (2SC) phases, are reviewed. The effect of a magnetic field on the pairing dynamics in two-flavor color-superconducting dense quark matter is investigated. A universal form of the gap equation for an arbitrary magnetic field is derived in the weakly coupled regime of QCD at asymptotically high density, using the framework of Schwinger-Dyson equation in the improved rainbow approximation. The results for the gap in two limiting cases, weak and strong magnetic fields, are obtained and discussed. It is shown that the superconducting gap function in the weak magnetic field limit develops a directional dependence in momentum space. This property of the gap parameter is argued to be a consequence of a long-range interaction in QCD.

ACKNOWLEDGEMENTS

First of all, I would like to gratefully acknowledge my advisor Dr. Igor Shovkovy for this thesis project. I thank him for introducing me to the research field of color superconductivity and innumerable stimulating discussions and suggestions. I have benefitted from his experience, his knowledge, and his patience. Without his support, there is no doubt that I could not complete this thesis.

Second, I would like to thank my group member Xinyang Wang. Through many discussions in a nice and friendly atmosphere, he helped me to understand a lot of the problems for this thesis.

Furthermore, I thank all professors who taught me physics courses: Prof. John Shumway, Prof. Kevin Schmidt, Prof. Mike Treacy and Prof. William Kaufmann. They helped me learn a lot of background knowledge in physics. My special thanks to Dr. Ricardo Alarcon and Dr. Richard Lebed for their help and support in the research work in the beginning years.

Thanks to my friends Qiyuan Wei, Xuan Ni and Yong Wei for the discussions and comments on many technical problems.

Finally, thanks to my parents for their understanding and encouragement.

TABLE OF CONTENTS

APPENDIX Page

LIST OF TABLES

LIST OF FIGURES

CHAPTER 1

INTRODUCTION

1.1 Dense Quark Matter

Quantum chromodynamics (QCD) is known to be the fundamental theory of strong interactions, which describes the interactions between quarks and gluons. It is a quantum field theory with the SU(3) Yang-Mills gauge symmetry [1], consisting of a system of color-charged fermions (the quarks) mediated by a set of exchange gauge bosons (the gluons). There are six types of quarks with spin of 1/2 known as flavors. They are called up, down, strange, charm, bottom, and top, and they carry fractional electric charges. Up, charm, and top quarks have a charge of +2/3, while down, strange, and bottom quarks have a charge of -1/3. Each flavor of quark is assigned to the fundamental representation (denoted $\mathbf{3}$) of the local SU$(3)_c$ color gauge group, carrying a color charge of red, green or blue. Every quark has an antiquark, which can take one of three anticolors, called antired, antigreen, and antiblue, and belongs to the antitriplet representation (denoted $\bar{\mathbf{3}}$) of SU$(3)_c$. The gluon, containing an octet of vector gauge fields, belongs to the adjoint representation (denoted $\mathbf{8}$) of SU$(3)_c$. The QCD theory is an important part of the Standard Model of particle physics, which was established by Glashow [2], Weinberg [3] and Salam [4].

QCD was derived from various remarkable experimental observations and gained a great successful interpretation for few-body phenomena of hadronic physics. For example, the evidence for quarks as real constituent elements of hadrons was obtained in deep inelastic scattering experiments at SLAC [5, 6], the evidence for gluons in three jet events at PETRA [7], the running of the QCD coupling [8], heavy-quark (charm, bottom, and top quarks) production in colliders [9, 10, 11, 12, 13], etc.

It is found that QCD has two important properties. One of them is color confinement, which means color charged particles (such as quarks) cannot be isolated as asymptotic states, and therefore cannot be directly observed. Because of this, quarks are forever bound into hadrons such as the proton and the neutron. Although analytically unproven, confinement is widely believed to be true because it explains the consistent failure of free quark searches in experiments. The other property of QCD is asymptotic freedom, which means that quarks and gluons interact very weakly in very high-energy reactions. This prediction of QCD was first discovered in the early 1970s by Politzer, Wilczek and Gross [14, 15]. It allows physicists to make precise predictions of the results of many high energy experiments using the quantum field theory technique of perturbation theory, such as the R ratio in e^+e^- annihilation [16].

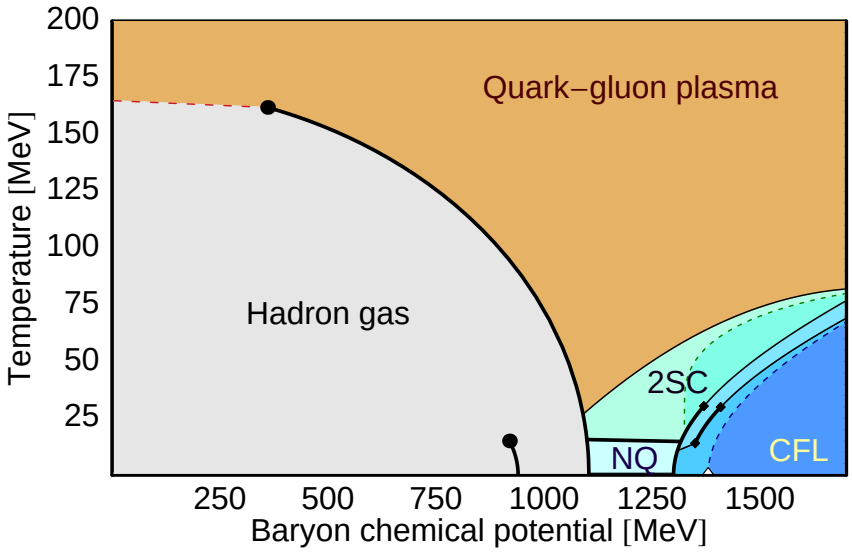

Figure 1.1: A schematic version of QCD phase diagram, adapted from Ref. [17].

The use of the QCD theory also allows to study the behavior of many-body systems of quarks, in the so-called regime of “condensed matter physics” of quantum chromodynamics [18]. Conventionally, we can explore the corresponding phase diagram in the plane of the temperature T and the baryon chemical potential

μ_B (see Fig. 1.1), and investigate the properties of different phases. (Note that the quark chemical potential is three times smaller than the baryon chemical potential, $\mu \equiv \mu_B/3$.) As we know, when temperatures and densities are both relatively low, quarks are confined into colorless hadronic degrees of freedom (such as mesons and baryons, which are bound states of quarks and antiquarks).

However, at sufficiently high temperatures or densities, the structure of the normal hadronic matter phase is disrupted: the hadrons are crushed into their constituent quarks. When this happens, the constituent quarks become deconfined and mobile over large distances. Therefore, it is more reasonable to select the quarks as the basic degrees of freedom instead of hadrons. The corresponding phase is called quark matter.

When the temperature is sufficiently high, i.e., larger than the QCD energy scale ($\Lambda_{QCD} \approx$ 200 MeV, or of order 10^{12} K), the phase of matter becomes a kind of hot quark matter called the quark-gluon plasma (QGP). This was the state of matter in the Early Universe when the Universe was only a few tens of microseconds old. Quark-gluon plasma can also be produced in small, short-lived regions of space by heavy-ion collisions at very powerful accelerators, such as RHIC at Brookhaven National Laboratory [19, 20] and LHC at the European Organization for Nuclear Research (CERN) [21].

When the temperature is close to zero and the quark chemical potential increases, as we can see from Fig. 1.1, there exists a phase transition from low-density hadronic matter (vacuum at $T \approx 0$) to nuclear matter. This occurs at a critical quark chemical potential μ about 310 MeV. Nuclear matter consists mainly of neutrons and some protons, interacting primarily by nuclear interactions (or residual strong interactions) but also slightly affected by electromagnetic interactions [22, 23]. If we continue increasing the quark density (or quark chemical po-

tential) and keep the temperature sufficiently low, compressed nuclear matter will make a transition to a phase of cold and dense quark matter. The critical quark chemical potential for the transition can be determined by comparing the equations of state of both nuclear matter and quark matter. However, while such equations of state are subject of many investigations, they are not fully established yet.

The topic of cold and dense quark matter has gained a lot of interest in physics because of its astrophysical significance in nature. It has been suggested for a long time that the interior of neutron stars is the only known place in the Universe where the baryon density might possibly be high enough and the temperature might be low enough for dense quark matter to exist. As we know, a typical neutron star has a mass of about $1.2 - 2.0$ solar masses [24] with a radius of about 10 km [25], which is about 1/60,000 of the Sun's radius. The weight of a neutron star is so large that it is compressed to an ultrahigh density by its gravity. In fact, the density of a neutron star varies from less than 1×10^9 kg/m^3 in the crust [26] and increases with depth to about 3-12 times the nuclear saturation density ($n_0 = 0.16$ nucleons/fm^3, or $\rho_0 = 2.8 \times 10^{17}$ kg/m^3) in the central region [27, 28]. In addition, neutron stars are born very hot in supernova explosions and their interior temperatures can reach up to about 10^{11} K (or 10 MeV). (Note that the surface temperature of neutron starts may be a few orders of magnitude smaller than the interior temperature.) However, the interior temperature drops to about 10^8 K (or 10 keV) rapidly by neutrino emission within a few years [25]. After a time of about a million years, the interior temperature of neutron stars can even cool down to 10^7 K (or 1 keV) [29].

Based on the above discussion of properties of neutron stars, we may expect to find quark matter in the cores of neutron stars. Furthermore, the cold and dense quark matter has been predicted to be a color superconductor [30, 31, 32, 33, 34], which is a degenerate liquid of quarks, with Cooper pairing near the Fermi

surface that spontaneously breaks the color gauge symmetry. A few seconds after the birth of neutron stars, when the interior temperature of neutron stars drops to less than about 10 MeV, it may already be appropriate to discuss the possibility of cold dense quark matter. At present, we do not know whether neutron stars have quark matter cores or not. Even assuming that compact stars do contain quark matter, we do not know whether that quark matter is in a color-superconducting phase or not. Therefore, in order to resolve this uncertainty, we need to study color superconductivity and to improve our understanding of how such a quark matter core could affect the observable behavior of neutron stars. In the next section, we discuss color superconductivity in more detail.

1.2 Color Superconductivity

It is a good starting point to assume that quarks at sufficiently high density and low temperature form a degenerate Fermi liquid. Such quarks have a tendency to form Cooper pairs (explicit reasons will be discussed in the next section). The first physicists to realize that Cooper pairing could occur in quark matter were Ivanenko and Kurdgelaidze in 1969 [35, 36], when the theory of the strong interaction was not even fully established. However, their insight was not pursued until the development of QCD in the early 1970s. In 1977 Barrois and Frautschi realized that QCD predicts Cooper pairing in high-density quark matter [30, 31, 32]. They were the first to use the term "color superconductivity". At around the same time the problem was also discussed by Bailin and Love [37], who studied various pairing patterns in detail. However, except for the papers by Iwaskai and Iwado in 1995 [38, 39], there was little activity in dense quark matter and color superconductivity until 1998, when the prediction of large pairing gaps was sparked by the simultaneously published work of two groups (Alford $et\,al.$ [40] and Rapp $et\,al.$ [41]). This suggested that the phenomenon of color superconductivity was much more significant than

it had previously been suggested. From then on, the phenomenology of color-superconducting quark matter has been widely studied and interest in the topic has steadily grown (for reviews, see [18, 42, 43, 44, 45, 46, 47, 48, 49, 50, 51, 52, 53, 54]). Based on the research in the past decade, we find that quark matter at the highest densities is the color-flavor-locked (CFL) color superconductor [55]. The corresponding ground state is such that up, down, and strange quarks participate in Cooper pairing on equal footing and most of the symmetries of the QCD Lagrangian remain unbroken. After CFL, in the intermediate density region, the simplest less symmetrically paired phase of quark matter is the two-flavor color-superconducting (2SC) phase [32, 40, 41, 42]. It contains quarks of only two flavors (up and down quarks) participating in Cooper pairing. The properties of both CFL and 2SC phases at asymptotic densities were rigorously calculated from first principles in the numerous papers [56, 57, 58, 59, 60, 61, 62, 63, 64]. There are two important features that guarantee rigorous calculations for both phases. One is the property of asymptotic freedom in QCD, which ensures that such matter is weakly interacting at asymptotically large densities and, therefore, allows a rigorous truncation of the Schwinger-Dyson (gap) equation. The other one is that the long-range QCD interactions are cut off by Landau damping and Debye screening effects in a dense medium [56, 65], which help to avoid usual infrared problems of QCD associated with strong coupling and essentially nonperturbative infrared dynamics.

There are many types of less symmetrically paired phases of quark matter in the intermediate density region between nuclear and CFL matter, where the densities may not be high enough for the perturbative calculations to be reliable. The only known alternative is the numerical computational approach of lattice QCD, which unfortunately has a technical difficulty (the "sign problem") [66]. Thus, it means that we have to use effective models for the moderate density region, such as the

Nambu-Jona-Lasinio (NJL) model [67, 68]. We shall discuss the properties of both CFL and 2SC phases in the following sections, and finally focus on the study of the 2SC phase.

1.3 Quark Cooper Pairing

Why should high-density and low-temperature quark matter be a color-superconducting phase? This is a straightforward prediction that follows from making an analogy with conventional superconducting metals. It is well known that at low temperatures many metals become superconductors. Electrons in metals are treated as a Fermi liquid. When below a critical temperature, the electrons near the Fermi surface gain an attractive phonon-mediated interaction, which causes them to pair up and form a condensate of Cooper pairs. This phenomenon is fully explained by the Bardeen-Cooper-Schrieffer (BCS) mechanism [69]. Interestingly, the same ingredients are also present in dense and cold quark matter, and they are realized even more straightforwardly. When densities are sufficiently high, the quarks near the Fermi surface are weakly interacting because of asymptotic freedom. The dominant strong interaction between quarks is the one-gluon exchange, which is attractive in its antisymmetric channel. In contrast, the dominant Coulomb interaction of electrons in superconducting metals is repulsive and the effective attractive interaction that governs superconductivity is mediated by phonons. The attraction leads to the formation of Cooper pairs. Therefore, it is natural to expect that color-superconducting phases should occur at sufficiently low temperature and high density. At asymptotic densities, the properties of color superconductivity can be rigorously and directly calculated from first principles.

Unlike a conventional superconductor, color-superconducting quark matter can form many different types of color-superconducting phases. It is because there

are three different colors (red, green, blue), and in the cores of neutron stars, which are not dense enough to contain any charm or heavier quarks, there are up to three different flavors (up, down, strange). Thus, in forming the Cooper pairs, there is a 9×9 color-flavor matrix of possible pairing patterns. To emphasize this difference, as well as the fact that quarks carry colors, superconductivity in quark matter is called *color superconductivity*. Generally, the quark-pair condensate can be characterized by the expectation value of the one-particle-irreducible diquark two-point function, also known as the anomalous self-energy,

$$\langle \psi^a_{i\alpha} \psi^b_{j\beta} \rangle = P^{ab}_{ij\alpha\beta} \Delta, \tag{1.1}$$

where ψ is the quark field operator. Color indices a, b range over red, green, and blue (r,g,b), flavor indices i, j range over up, down, and strange (u,d,s), and α,β are the spinor Dirac indices. The matrix $P^{ab}_{ij\alpha\beta}$ specifies a particular color-flavor-Dirac pairing channel, and Δ is the gap parameter which gives the strength of the pairing in this channel. From this definition, in order to understand properties of color superconductivity, obviously, we need to analyze the color-flavor-Dirac structures for different patterns of pairing and calculate the gap parameters for different channels.

At present, many different phases of quark matter have been proposed. There is no certainty that all possibilities have already been exhausted [70]. As we have mentioned above, in the limit of asymptotically large density, the favored ground color-superconducting phase is the color-flavor-locked phase (CFL), which is a kind of three-flavor quark matter. When densities become lower and the mass of the strange quark cannot be ignored compared with the masses of up and down quarks, another pattern of pairing, the so-called two-flavor superconducting (2SC) phase is proposed. Now we begin to discuss what kind of color-flavor-Dirac structure is favored for the CFL and 2SC phases. For simplicity, other possible phases of color superconductivity at lower densities will not be discussed here.

The quark field belongs to the fundamental representation of the SU$(3)_c$ group. Group-theoretically, after pairing two quarks (color triplets), we can find that there are two inequivalent color structures of diquark states possible, $\mathbf{3} \otimes \mathbf{3} = \bar{\mathbf{3}}_A \oplus \mathbf{6}_S$. The color antisymmetric anti-triplet ($\bar{\mathbf{3}}_A$) channel is favored, because it is the most attractive channel for quarks interacting via single-gluon exchange. This is the dominant interaction at high densities, where the QCD coupling is weak.

The color tensor for the quark-quark scattering amplitude in the one-gluon exchange approximation is given by the following structure:

$$\sum_{A=1}^{N_c^2-1} T^A_{aa'} T^A_{b'b} = -\frac{N_c+1}{4N_c}(\delta_{aa'}\delta_{bb'} - \delta_{ab'}\delta_{a'b}) + \frac{N_c-1}{4N_c}(\delta_{aa'}\delta_{bb'} + \delta_{ab'}\delta_{a'b}). \quad (1.2)$$

The first antisymmetric term in Eq. (1.2) corresponds to the attractive antitriplet channel, while the second symmetric term corresponds to the repulsive sextet channel. It was found that Cooper pairing in the symmetric sextet channel does not break any additional symmetries and is still induced, but remains much weaker than that in the antisymmetric antitriplet channel [55, 62, 71, 72]. Therefore, the contribution of this subdominant pairing is generally neglected in most considerations. It should be noted that the antisymmetric channel is also the most attractive channel for quarks interacting via the instanton-induced 't Hooft interaction, which is important at lower densities [40, 41].

Next, as we know, a conventional BCS condensate of Cooper pairing is a spin singlet, with a total zero momentum (two quarks with equal and opposite momentum). It is the simplest spin structure for the pattern of Cooper pairing, which is realized in the case of the CFL and 2SC superconducting phases. Therefore, for these two phases, the Dirac structure $\psi^T C\gamma^5\psi$ is introduced, which is a Lorentz scalar and corresponds to parity-even spin-singlet pairing. A scalar condensate is favorable because it leaves rotational invariance unbroken and its pair-

ing is stronger, compared with the channels that break rotational symmetry [39, 55, 73, 74, 75, 76]. As for a similar spin-0 condensate $\psi^T C\psi$ without γ^5, it is a pseudoscalar with negative parity, which is disfavored in QCD because of the instanton effects [41, 55, 77].

Since the condensate is required to be antisymmetric in color and in Dirac indices, it should be antisymmetric in flavor indices to be in agreement with the Fermi-Dirac statistics and the Pauli exclusion principle. Therefore, the most general color-flavor-Dirac structure for the CFL and 2SC phases is

$$\langle \psi_i^a C\gamma^5 \psi_j^b \rangle \propto \gamma^5 \epsilon^{abA} \epsilon_{ijB} \phi_B^A \Delta, \tag{1.3}$$

where the Dirac structure is unambiguously fixed by demanding a positive-parity state. Let us now discuss the color-flavor structure in the following. However, because of the number of the quark flavors participating in pairing, they have obviously different pairing patterns and properties. And in the next sections we will discuss them separately.

In addition to the symmetry properties indicated by color-flavor structures, another important feature of color superconductivity in dense quark matter is the appearance of a non-zero energy gap in the quark quasiparticle spectrum. The corresponding expression for the energy reads

$$\varepsilon_k = \sqrt{(E_k - \mu)^2 + \Delta^2}, \tag{1.4}$$

where $\boldsymbol{k}$ and Δ are the momentum and the gap in the quasiparticle energy, respectively, and $E_k = \sqrt{\boldsymbol{k}^2 + m^2}$ with $k = |\boldsymbol{k}|$. The presence of the gap in the energy spectrum should affect transport and thermodynamic properties. For example, conductivities, viscosities, neutrino emissivity and specific heat are suppressed by the exponentially small factor $\exp(-\Delta/T)$ at small temperature, $T \ll \Delta$ [78, 79, 80, 81, 82, 83].

In general, different patterns of color superconductivity have different properties and lead to different effects in neutron stars. So it is of great phenomenological interest to perform a systematic study to sort through all possible phases and investigate their properties. Then, by comparing with observable astrophysical signatures, we can decide which specific color-superconducting phases are favored or disfavored empirically.

In the following, the properties of two simplest pairing patterns, the CFL and 2SC phases, will be reviewed in more detail.

1.4 CFL Phase

The CFL pairing pattern [55], corresponding to $\phi_B^A = \delta_B^A$ in Eq. (1.3), is given by

$$\langle \psi_i^a C\gamma^5 \psi_j^b \rangle \propto \Delta_{\mathrm{CFL}} \epsilon^{abA} \epsilon_{ijA} \gamma^5. \tag{1.5}$$

It is antisymmetric in color and flavor indices, which both run from 1 to 3. This is the only pattern that pairs all three colors and all three flavors on equal footing to form conventional zero-momentum spinless Cooper pairs at ultrahigh densities, where the effects of the strange quark mass can be neglected and thus the up, down, and strange quarks can be treated equally. Note that the subdominant term from an induced Cooper pairing, which is symmetric in color and flavor indices, is ignored in Eq. (1.5). Its inclusion, however, does not affect any qualitative features of the CFL phase.

To large extent, the symmetry breaking pattern for the CFL phase is determined by the color and flavor structure of the diquark condensate of Cooper pairs in Eq. (1.5). We find that the symmetry of QCD Lagrangian density is broken as follows:

$$\mathrm{SU}(3)_c \times \mathrm{SU}(3)_L \times \mathrm{SU}(3)_R \times \mathrm{U}(1)_B \to \mathrm{SU}(3)_{c+L+R} \times \mathbb{Z}_2. \tag{1.6}$$

With all quarks assumed to be massless, the QCD Lagrangian density possesses the global $\mathrm{SU}(3)_L \times \mathrm{SU}(3)_R$ chiral symmetry and the global $\mathrm{U}(1)_B$ symmetry connected with the baryon number conservation. In the presence of the CFL pairing, the condensate breaks the $\mathrm{SU}(3)_c$ color gauge symmetry and $\mathrm{SU}(3)_L \times \mathrm{SU}(3)_R$ chiral symmetry, leaving only the diagonal subgroup $\mathrm{SU}(3)_{c+L+R}$ unbroken. Because of the contraction over a common index A in Eq. (1.5), which is connecting color and flavor indices, the condensate is not invariant under color rotations, nor under flavor rotations, but only under simultaneous, equal and opposite, color and flavor rotations. The CFL condensate pairs left-handed quarks with each other only and right-handed quarks with each other only. The color and chiral symmetries are broken by locking of color and flavor rotations to each other for these two separate condensates. This mechanism is called locking, and the corresponding phase of matter is called color-flavor-locked (CFL) phase [55]. It is quite different from the quark-antiquark condensate that breaks chiral symmetry in the vacuum by pairing left-handed quarks with right-handed antiquarks. The matrix of electric charges $Q_f = \mathrm{diag}(2/3, -1/3, -1/3)$ in flavor space is one of the generators of $\mathrm{SU}(3)_L \times \mathrm{SU}(3)_R$ group, which generates the $U(1)_{em}$ gauge symmetry. In the CFL ground state, there is also a gauged generator $\tilde{Q}$, which corresponds to an unbroken $\tilde{U}(1)_{em}$ gauge symmetry. Its transformations consist of simultaneous electromagnetic and color rotations. The unbroken rotated photon $\tilde{A}_\mu$, which is a linear combination of the original photon A_μ, the 3th gluon A^3_μ and the 8th gluon A^8_μ, i.e., $\tilde{A}_\mu = \frac{gA_\mu - eA^3_\mu - \frac{e}{\sqrt{3}}A^8_\mu}{\sqrt{g^2 + \frac{4e^2}{3}}}$ [84, 85], remains massless, and thus experiences no Meissner effect. Here, e and g are the QED and QCD couplings. The rest of the gluons and the orthogonal gluon-photon combination become massive as a result of the color Meissner effect. This is quite different from the conventional superconducting metals, where photons become massive due to electromagnetic Meissner effect and are expelled by a superconductor. Since the corresponding generator of the

rotated charge $\tilde{Q}$ remains unbroken, every diquark in the condensate should have $\tilde{Q} = 0$. The explicit expression for $\tilde{Q}$ in the CFL phase reads

$$\tilde{Q} = Q_f \otimes I_c - I_f \otimes (T_3)_c - I_f \otimes (\frac{T_8}{\sqrt{3}})_c, \tag{1.7}$$

where T_3 and T_8 are the 3th and 8th generators of $\mathrm{SU}(3)_c$ gauge group in the adjoint representation. In units of $\tilde{e} = \frac{eg}{\sqrt{g^2+\frac{4e^2}{3}}}$, the $\tilde{Q}$ charges of quarks in the CFL phase are given in Table 1.1.

Table 1.1: $\tilde{Q}$ charges of quarks in the CFL phase.

u_r	u_g	u_b	d_r	d_g	d_b	s_r	s_g	s_b
0	+1	+1	-1	0	0	-1	0	0

By evaluating the color-flavor structure of the condensate explicitly for the CFL phase, in such a ground state with the $\mathrm{SU}(3)_{c+L+R}$ symmetry, the original nine quark states give rise to a singlet and an octet of quasiparticles. The gap matrix can be rewritten as follows [55, 62, 63]

$$\Delta^{ij}_{ab} = i\gamma^5 \left[\frac{1}{3}(\Delta_1 + \Delta_2)\delta^i_a\delta^j_b - \Delta_2\delta^i_b\delta^j_a\right], \tag{1.8}$$

where Δ_1 is the gap of the singlet Cooper pair, while Δ_2 is the gap of the octet Cooper pairs. The octet condensates include u_g-d_r, d_b-s_g, u_b-s_r pairs, as well as two linear combinations of the pairs made of the three quarks u_r, d_g, and s_b. The singlet condensate is the remaining orthogonal combination of u_r, d_g, and s_b. When a small symmetric diquark condensate is neglected, one finds that $\Delta_1 = 2\Delta_2$, i.e., the gap of the singlet is twice as large as the gap of the octet. Since all quasiparticles are gapped in the diquark condensates with zero net $\tilde{Q}$ charge, the CFL phase is a transparent insulator at sufficiently low temperature [86, 87]. At small temperatures its electrical conductivity is dominated by thermally excited electrons and positrons [86].

It appears that the CFL pairing condensate spontaneously breaks the exact global $\mathrm{U}(1)_B$ baryon number symmetry, leaving only a discrete $\mathbb{Z}_2$ symmetry. According to the Goldstone theorem, the breaking of baryon number symmetry will result in the appearance of a massless Goldstone boson that makes the CFL phase a superfluid [88]. As a consequence, if the CFL quark matter appears in a core of a rotating compact star, it will be threaded with rotational vortices, which have been studied in Refs. [89, 90, 91, 92].

After briefly discussing the symmetry breaking and properties associated with the color-flavor structure, one important feature of the CFL phase left out is the gap parameter, which can be determined analytically by solving the gap equation at asymptotic densities. This is discussed in detail in the Appendix A, where explicit derivation of the gap equation and the calculation of gap parameter in the 2SC phase are given. Similar results are also valid for the gaps in the CFL phase [62, 63, 64].

1.5 2SC Phase

Now, let us turn to the discussion of the properties of the 2SC phase. This is a color-superconducting phase with Cooper pairs including only up and down quarks. By taking $\phi_B^A = \delta_3^A \delta_B^3$ in Eq. (1.3), the color-flavor-Dirac structure of the 2SC phase is given by

$$\langle \psi_i^a C\gamma^5 \psi_j^b \rangle \propto \Delta_{2\mathrm{SC}} \epsilon^{ab3} \epsilon_{ij3} \gamma^5. \tag{1.9}$$

From the structure in Eq. (1.9), we can find that only quarks with two (red and green) out of three colors participate in the Copper pairing of the 2SC phase, while quarks with the third (blue) color are unpaired. In other words, the original six quark states give rise to two doublets of gapped quasiparticles and two unpaired quasiparticles (singlets with respect to the $\mathrm{SU}(2)_c$ unbroken gauge group). The

Copper pair condensates involve the combinations of u_r-d_g and u_g-d_r only. It should be noted that the color indices in Eq. (1.9) may have an arbitrary orientation in the color space, since it can be changed by the global color transformations. We choose the condensate to point to in the third (blue) color direction by convention. Based on the color-flavor structure for the 2SC phase, the corresponding symmetry breaking pattern is

$$\mathrm{SU}(3)_c \times \mathrm{U}(1)_B \to \mathrm{SU}(2)_c \times \mathrm{U}(1)_{\tilde{B}}. \tag{1.10}$$

If the masses of up and down quarks are neglected, the global $\mathrm{SU}(2)_L \times \mathrm{SU}(2)_R$ chiral symmetry present in two-flavor QCD is not broken in the 2SC phase. As a consequence of the condensate pointing in the antiblue color direction, see Eq. (1.9), the color $\mathrm{SU}(3)_c$ gauge symmetry is broken down to the $\mathrm{SU}(2)_c$ color gauge subgroup. Therefore, five out of total eight gluons of $\mathrm{SU}(3)_c$ gauge group become massive due to the Meissner effect, while the other three gluons, corresponding to the unbroken $\mathrm{SU}(2)_c$ gauge group, remain massless. Although the original $\mathrm{U}(1)_B$ baryon number symmetry in vacuum is broken in the 2SC phase, a new rotated $\mathrm{U}(1)_{\tilde{B}}$ baryon number symmetry in medium remains unbroken. This means that the quark matter in the 2SC phase, unlike the CFL phase, is not superfluid. The corresponding generator $\tilde{B}$ of the baryon number symmetry, is a linear combination of the original baryon number B and the broken 8th gluon generator T_8 of $\mathrm{SU}(3)_c$ color gauge group. Its explicit form reads

$$\tilde{B} = B - \frac{2}{\sqrt{3}} T_8. \tag{1.11}$$

As is easy to check, the red and green quasiparticles participating in Cooper pairing carry zero baryon number, while the blue unpaired ones carry a non-zero value.

Similar to the CFL phase, there is an unbroken $\tilde{U}(1)_{em}$ gauge symmetry in 2SC phase too. The corresponding rotated electromagnetic gauge field $\tilde{A}_\mu$

is a linear combination of the vacuum photon A_μ and the 8th gluon A_μ^8: $\tilde{A}_\mu = \cos\theta\, A_\mu - \sin\theta\, A_\mu^8$, where $\cos\theta = g/\sqrt{g^2 + e^2/3}$ [84, 85]. Since $e \ll g$, the angle θ is close to zero, meaning that the rotated photon $\tilde{A}_\mu$ is mostly the original photon A_μ with a small admixture of gluon A_μ^8. Although both the vacuum photon A_μ and the 8th gluons A_μ^8 become massive via the Meissner effect because of the Higgs mechanism, the rotated photon $\tilde{A}_\mu$ is not subject to the electromagnetic Meissner effect and stays massless. The orthogonal gluon-photon combination, $\tilde{A}_\mu^8 = \sin\theta\, A_\mu + \cos\theta\, A_\mu^8$, which underlies the color Meissner effect, is still massive. The unbroken charge generator $\tilde{Q}$ for the 2SC phase is defined as follows:

$$\tilde{Q} = Q_f \otimes I_c - I_f \otimes (\frac{T_8}{\sqrt{3}})_c, \tag{1.12}$$

where $Q_f = \text{diag}(2/3, -1/3)$ is the matrix of electromagnetic charges of u and d quarks in flavor space. Thus, by using Eq. (1.12), we can easily find the $\tilde{Q}$ charges for quasiparticles in the 2SC phase (see Table 1.2), in units of $\tilde{e} = e\cos\theta$.

Table 1.2: $\tilde{Q}$ charges of quarks in the 2SC phase.

u_r	u_g	u_b	d_r	d_g	d_b
$+\frac{1}{2}$	$+\frac{1}{2}$	+1	$-\frac{1}{2}$	$-\frac{1}{2}$	0

The situation in 2SC phase is not exactly the same as the CFL phase with respect to the $\tilde{U}(1)_{em}$ gauge symmetry. Because of the presence of the unpaired blue quarks with non-zero $\tilde{Q}$ charge, the 2SC phase is a conductor, not an insulator. In addition, if unpaired massive strange quarks are also included in the 2SC phase, an additional approximate $\mathrm{U}(1)_S$ global symmetry can be introduced [54], which is unbroken by the 2SC pairing.

After investigating the symmetry properties, determined by the color-flavor structure of the condensate, we turn to the discussion of the properties related to

the gap parameter Δ. As we have mentioned in the last section, the magnitude of the gap can be obtained rigorously from first principles for the 2SC and CFL phases at asymptotic densities by making use of the self-consistent gap equation. Conventionally, the gap equation is derived in the framework of the Schwinger-Dyson equation, and usually the derivation of explicit expressions for the quark and gluon propagators is needed before solving it. All such derivations are presented in Appendix A and the solution for the gap parameter is also given.

1.6 Neutrality, β Equilibrium and Mass Effects

In the above sections, we have discussed the main properties of two simplest possible color-superconducting phases in cold and dense quark matter. It should be emphasized, that the above arguments for the formation of quark Cooper pairs are based on one idealized assumption that the pairing quarks have same chemical potentials. It may be a good assumption at the asymptotically large densities. However, this is not the real situation that can be realized in the interior of the neutron stars, where $n \lesssim 10 n_0$, and the value of the quark chemical potential cannot be much larger than 500 MeV. At such moderate densities, it is found that the quark mass, combined with β equilibrium and neutrality requirements, may modify the quark chemical potentials for different quark colors and flavors. Consequently, an extra energy cost ("stress") will be imposed on the formation of Cooper pairs.

Here, to explain this effect, we discuss a simplified example: two massless species of quarks, labeled 1 and 2, have different chemical potentials μ_1 and μ_2. Let the gap parameter associated with Cooper pairing be Δ. We define the average chemical potential and the mismatch parameter as

$$\begin{aligned} \bar{\mu} &= \frac{\mu_1 + \mu_2}{2}, \\ \delta\mu &= \frac{\mu_1 - \mu_2}{2}. \end{aligned} \tag{1.13}$$

The quasiparticle dispersion relation in the corresponding color-superconducting phase is given by [93, 94],

$$\varepsilon_k = |\sqrt{(k-\bar{\mu})^2 + \Delta^2} \pm \delta\mu|. \tag{1.14}$$

For $\delta\mu < \Delta$, pairing between species 1 and 2 leads to a gapped energy spectrum. A qualitative change appears at $\delta\mu = \Delta$, where the spectrum becomes gapless at momentum $k = \bar{\mu}$. For $\delta\mu > \Delta$, the dispersion relations become gapless at the two values of momenta

$$k_\pm = \bar{\mu} \pm \sqrt{\delta\mu^2 - \Delta^2}. \tag{1.15}$$

It means that there are quasiparticles with vanishingly small energies on two spheres in momentum space. In this case, due to the difference of quark chemical potentials for pairing quarks, the formation of Cooper pairs may be substantially modified, or even prevented, and thus the properties of quark matter can be influenced. Below, we discuss in detail how neutrality, β equilibrium and nonequal quark masses affect the Cooper pairing in the quark matter.

Neutrality Constraints

First, let us discuss the effect of charge neutrality on color superconductivity. From general considerations, stable matter in the bulk must be neutral under all gauged charges, whether they are spontaneously broken or not. Otherwise, the net charge density would create large fields, making the energy grow as a nonextensive quantity. To avoid such a large energy price, the charge neutrality should be satisfied with a very high precision.

For the electromagnetic gauge field, this simply requires zero electric charge density (at least, on average), $n_Q = 0$. But how does this condition make any constraint on quark matter? We can take a bulk of two-flavor quark matter, such as

the 2SC phase, as an example. Since the magnitude of the positive charge of the up quark (Q_u =+2/3) is twice as large as that of the negative charge of the down quark (Q_d = -1/3), we can find that the number density of down quarks should be approximately twice as large as number density of up quarks when considering no electrons, $n_d \approx 2n_u$. It is derived from charge neutrality straightforwardly, $n_Q = Q_u n_u + Q_d n_d \approx 0$. This then requires that $\mu_d \approx 2^{1/3}\mu_u$, i.e., μ_d is considerably larger than μ_u. Adding electrons (as required by β equilibrium, see the next subsection) changes the relation slightly, but the qualitative result will be approximately the same.

Similarly, the color charge neutrality should be imposed. The correct formal requirement concerning the color charge of a large lump of matter is that it should be a color singlet because of the color confinement in the real world. It means a state invariant under a general color gauge transformation. However, in phenomenological models, it is sufficient for us to impose color neutrality, meaning equality in the numbers of red, green, and blue quarks, which is a less stringent constraint compared with the requirement of a color singlet. Usually, there exist two mutually commuting color charges Q_3 and Q_8 for the quark matter, which are related to the generators T_3 and T_8 of the SU(3)$_c$ gauge group. So we need to impose the charge densities of Q_3 and Q_8 to be zero, $n_3 = n_8 = 0$.

Generally speaking, in order to enforce the color and electric neutrality in the theoretical study of the color-superconducting ground state, for example, in the NJL model, one could introduce an electron chemical potential μ_e and two independent chemical potentials for the corresponding two color charges μ_3 and μ_8 by hand, and then find the extremum of the thermodynamic potential Ω (or "free energy") with respect to these chemical potentials. This is implemented as follows. The common quark chemical potential μ in the Lagrangian density is replaced by a chemical

potential matrix $\hat{\mu}$ for different quarks in color-flavor space, e.g., see Eq. (2.3) below. The corresponding neutrality conditions are

$$\begin{aligned} n_Q &= \frac{\partial \Omega}{\partial \mu_e} = 0, \\ n_3 &= -\frac{\partial \Omega}{\partial \mu_3} = 0, \\ n_8 &= -\frac{\partial \Omega}{\partial \mu_8} = 0. \end{aligned} \tag{1.16}$$

Making use of these color and electric charge neutrality conditions, the values of μ_e, μ_3 and μ_8 can be obtained. Different color and flavor quarks will generally have non-equal chemical potentials.

β Equilibrium

It was mentioned that neutrino emission due to the β processes plays an important role in the cooling of neutron stars. The matter in the bulk of a neutron star should also remain in β equilibrium. It means that all β processes, such as $d \to u + e^- + \bar{\nu}_e$ and $u + e^- \to d + \nu_e$, should go with equal rates in both directions. Note that the neutrinos are not in equilibrium because they have large mean free path and leave the star after been produced. Consequently, the chemical potentials of different quarks must satisfy some relations and give rise to some mismatch. For example, in the case of two-flavor quark matter, the chemical potentials of the up quark and the down quark, μ_u and μ_d, should satisfy the relation $\mu_d = \mu_u + \mu_e$, where μ_e is the chemical potential of electrons. It is clear that the chemical potential mismatch for up and down quarks is $\delta\mu = \frac{\mu_d - \mu_u}{2} = \frac{\mu_e}{2}$. As we have discussed above, the introduction of μ_e is required for enforcing electric charge neutrality in the color-superconducting ground state. Therefore, when the charge neutrality and the β equilibrium in two-flavor quark matter are enforced, a stress on the formation of Cooper pairs is imposed. In turn, additional complications arise for Cooper pairing. For example, if $\delta\mu > \Delta$, the ground state of two-flavor quark matter is given by so

called gapless 2SC phase (g2SC), not 2SC phase, whose properties in the low-energy region are similar to those in the normal phase. For more details about g2SC phase, see Refs. [93, 94].

Quark Mass Effects

At intermediate densities, when the mass of strange quark cannot be neglected, we extend the above arguments to include the leading effects of nonequal quark masses. It is found that the difference in the masses of the pairing quarks gives rise to different Fermi momenta even when the chemical potentials are the same. This, in turn, results in different effective chemical potentials for quarks. Thus, again a stress on the BCS pairing could arise. As we know, the current masses m_u and m_d of the light up and down quarks are of the order of about 5 MeV, and the current mass m_s of the strange quark is approximately 90 MeV. In the vacuum, the constituent quark masses of up and down are about 300 MeV, while the constituent strange quark mass is of the order of 500 MeV. However, the constituent quark masses are expected to decrease with increasing quark density. Therefore, most likely, the actual medium-modified values of quark masses in dense matter should be in the range between the current masses and the constituent quark masses, i.e., between about 5 MeV and 300 MeV for up and down quarks, and between about 90 MeV and 500 MeV for strange quarks. Consequently, the mass of strange quark M_s at the densities in the neutron stars, where the typical value of the quark chemical potential, $\mu \simeq$ 500 MeV, is not negligible and is much larger than the masses of up and down quarks, M_u and M_d. (Here we denote the density-dependent constituent masses as M_u, M_d and M_s). In application to quark matter, the effect of the strange quark mass can lead to a reduction of the strange Fermi momentum,

$$k_F^s = \sqrt{\mu^2 - M_s^2} \simeq \mu - \frac{M_s^2}{2\mu}. \tag{1.17}$$

We see that the strange quark mass leads to a reduction in the quark chemical potential by a value of $\frac{M_s^2}{2\mu}$. We can write this as $\mu_s^{\rm eff} = \mu - \frac{M_s^2}{2\mu}$, when μ_e, μ_3 and μ_8 are ignored. This quantity plays the role of a mismatch parameter in three flavor quark matter, which is similar to $\delta\mu = \frac{\mu_e}{2}$ in two-flavor quark matter. For the same reason, this mismatch should interfere with Cooper pairing between strange and non-strange quarks. And it was shown in Ref. [95] that the CFL phase becomes gapless when $\delta\mu = \frac{M_s^2}{2\mu} > \Delta$, which is the so-called gCFL phase. Moreover, the stress arising from the strange quark mass will become more severe as the quark density (or the quark chemical potential μ) decreases, since the constituent mass of the strange quark will increase at the same time.

1.7 Color Superconductivity in Neutron Stars

As we have mentioned in Sec. 1.1, the central regions of a neutron star may be the only places allowing for color-superconducting quark matter. However, at present we have not observed anything that unambiguously suggests the existence of the color-superconducting phases in the cores of neutron stars. We cannot prove or discard its existence. Therefore, it is of great phenomenological interest to find out whether color superconductivity exists in the interior of neutron stars or not, and if it exists, what kind of color-superconducting phases or mixed phases with several color-superconducting components are favored at realistic neutron star densities. To this end, we need to explore theoretically all possible color-superconducting phases and their properties in detail. Then, we also need to understand their possible effects on the astrophysical observables from neutron stars. Finally, by comparing with the actual astrophysical observations, we can try to confirm or rule out the presence of color-superconducting phases in nature.

Before turning to the astrophysical signatures of quark matter in neutron star cores, we need to know physical properties extracted from experimental observa-

tions. These include the mass, radius, surface and/or interior temperature, rotation period and magnetic field. All these quantities of the neutron stars can be deduced by analyzing the spectra and frequency of the radiation pulses. And these characteristics could impose constraints on the properties of quark-matter phases.

The typical values for mass and radius have been quoted above in Sec. 1.1, and the measurement of them for many neutron stars has been made for a long time. The "mass-radius relation" gained from known neutron star data would yield a strong constraint on the equation of state of dense matter and, therefore, it is a good starting point to explore the quark-matter equation of state. Currently, model-parametric representations of the equation of state of dense quark matter are available for some color-superconducting phases, for example, the CFL phase [96] and the 2SC phase [97, 79, 98]. Under certain conditions, color superconductivity may have a large effect on the phase transition from nuclear matter to quark matter [99] and even on the properties of neutron stars [73]. Besides, such equations of state are the key input in the Tolman-Oppenheimer-Volkoff equations [100, 101] which determine the interior structure of compact stars. The presence of the gap parameter Δ arising from color superconductivity in those equations may modify theoretical predictions for the mass-radius relations. A recent precise measurement for the neutron star PSR J1614.2230 [102], yielded a mass of $1.97 \pm 0.04 M_{\odot}$ ($M_{\odot}$, solar mass). This is known be the highest value of neutron stars so far [24]. Such a high mass value imposes strong constraints on the properties of quark matter in the interiors of neutron stars, but does not exclude the possibility altogether [103]. General information about the temperature evolution of the neutron stars has been given in Sec. 1.1. As suggested by Fig. 1.1, temperatures present in old neutron stars are certainly lower than the estimated critical temperatures of color superconductors. But how can one determine whether color-superconduting quark matter is favored

and which color-superconduting phase is favored in the cores of neutron stars from the measurement of temperatures? Actually, the cooling process of the neutron stars is one of observational signatures that has the potential to differentiate various quark-matter phases. As we know, for neutron stars with ages ranging from tens of seconds to millions of years, the loss of energy is dominated by neutrino emission. Of course, generally, there is another factor related to the the decrease of temperature in the neutron star, the specific heat. Thus, by the measurements of the temperature and age of neutron stars, neutrino emissivity and specific heat can be obtained. On the other hand, different patterns of color-superconduting phases break different symmetries of the underlying theory, leading to different rates of neutrino emission and the specific heat, which are also different from the normal quark-matter phase. Consequently, the cooling rate of the neutron stars gives rise to the possibility to distinguish one phase from another. For example, as we have mentioned in previous sections, at small temperatures, the gapless quasiparticles in the 2SC phase, blue up and blue down quarks, give dominant contributions to the specific heat, as well as to the electrical and heat conductivities. Also, the presence of these ungapped quasiparticles should result in a large neutrino emissivity due to the β-processes. As for the gapped quarks with red and green colors, because of the presence of the gap Δ in the dispersion relations, the contributions of these gapped quasiparticles to transport and thermodynamic properties are suppressed by the exponentially small factor $\exp(-\Delta/T)$. This means the cooling rate of the 2SC phase is dominated by unpaired quarks. Meanwhile, for the CFL phase, in which all quark quasiparticles are gapped, their contributions to the cooling process are suppressed for the same reason. The Goldstone bosons, arising from the breaking of the $\mathrm{U}(1)_B$ baryon number symmetry and the chiral symmetry breaking, turn out to play an important role in neutrino emissivity and specific heat [104, 105]. And these quantities are many orders of magnitude smaller than those by unpaired

quarks, for example, the blue up and blue down quarks in the 2SC phases. This means that if a neutron star has a CFL core, the core holds little heat and emits few neutrinos, but is a good heat conductor (actually, all forms of dense matter are good heat conductors [79]) and so stays at the same temperature as the rest of the star. The rest of the star controls how the star cools. Obviously, this shows a difference between CFL quark matter and other color-superconducting phases.

Another important applicable astrophysical signature is associated with the rotation periods of the neutron stars. Neutron stars rotate extremely rapidly after their creation due to the conservation of angular momentum. Their rotation periods are between about 1 ms to 10 seconds [29]. Over time, neutron stars slow down because their rotating magnetic fields radiate energy. It is very interesting that observations have shown that the spinning-down of the star is interrupted by sudden spin-ups, called glitches. One possible explanation in Ref. [106] is that it may be related to the presence of a superfluid matter in some region of the neutron star. Briefly speaking, if a superfluid appears in a core of a rotating star, it will be threaded with rotational vortices. And then the glitches may be caused by occasional releasing of the angular momentum of rotational vortices, that remained pinned to the stellar crust. This may be the case for the CFL phase, as we have discussed in Sec. 1.4, which is a superfluid because of the breaking of baryon number symmetry.

Finally, we turn to the magnetic field of the neutron stars. From indirect measurements, the surface magnetic fields can reach up to about $B \simeq 10^{12}$ G [107, 108, 109]. For magnetars, the corresponding fields can be still a few orders of magnitude larger, i.e., $B \sim 10^{14} - 10^{15}$ G, and perhaps even as high as 10^{16} G [110]. Furthermore, it is possible that the magnetic field in the stellar interiors are much higher and reach up to about $B \sim 10^{18}$ G [107, 108, 109, 111]. Recently, the study of color superconductivity in the presence of magnetic fields attracted a

lot of attention [112, 113, 114, 115, 116, 117, 118, 119, 120, 121]. This interest is primarily driven by potential astrophysical applications, where magnetic fields play an important role. In the following main text of this thesis, we will concentrate on study of the properties of color superconductivity in magnetic fields, and especially, try to investigate how the magnetic fields modify the gap parameter of the 2SC phase.

CHAPTER 2

COLOR SUPERCONDUCTIVITY IN MAGNETIC FIELD

2.1 Introduction

In order to understand the properties of two- and three-flavor color-superconducting phases with spin-zero pairing in a magnetic field, it is important to first recall their electromagnetic properties. Despite being color superconductors, these phases can be penetrated by long-range "rotated" magnetic fields, which are not subject to the Meissner effect [84, 85]. The rotated gauge fields are linear combinations of the vacuum photon and one of the gluons. While all Cooper pairs are neutral with respect to the corresponding "rotated" electromagnetism, the individual quark quasiparticles carry well defined charges. It is not surprising, therefore, that the diquark pairing dynamics is affected by the presence of a magnetic field. The recent studies revealed many interesting qualitative features of the magnetic 2SC and CFL phases [112, 113, 114, 115, 116, 117, 118]. However, all such studies share a common shortcoming: they are performed in the framework of Nambu-Jona-Lasinio (NJL) models with contact interactions.

In this work we extend the analysis of two-flavor color superconductivity in a magnetic field by taking into account the long-range interaction in quark matter [122]. In particular, we perform the study in the framework of the Schwinger-Dyson equation for the gap function in the weakly-coupled regime of QCD at large densities. The long-range interaction is provided by the one-gluon exchange, in which the dominant screening and Landau damping effects are included. Our study reveals a qualitatively new feature of the magnetic 2SC phase, a directional dependence of the gap function, which is a consequence of the nonlocal interaction in the quark matter.

In the weak magnetic field limit, we find that the effect of a nonzero field can be mimicked by an effective increase of the strong coupling constant that governs the Cooper pairing dynamics: $g^2 \to g^2(1+\epsilon\sin^2\theta_{Bk})$, where θ_{Bk} is the angle between the quasiparticle momentum and the direction of the magnetic field, and the dimensionless quantity ϵ is a measure of ellipticity of the gap function. The latter is given by the dimensionless ratio $\epsilon = 27\pi(eB)^2/(2g^2\bar{\mu}^4)$, where B is the magnetic field and $\bar{\mu}$ is the quark chemical potential. As one can easily check, this ratio is much less than 1 even for the strongest possible fields in stars and, therefore, the use of the weak magnetic field limit is justified for all stellar applications. For completeness, we extend our analysis to the case of superstrong magnetic fields and find that the value of the gap increases with the field also in this regime. As expected on general grounds, the effects of non-locality of the interaction become negligible in superstrong fields and the directional dependence of the gap disappears. It should be remarked, however, that our analysis in the case of strong fields is performed with less rigor because the gluon screening effects in this case are not well known.

2.2 Model

As stated in Introduction, the analysis in this study is done in the framework of weakly-interacting two-flavor QCD at large densities. The quadratic part of the corresponding Lagrangian density of quarks in an external rotated magnetic field is given by

$$\mathcal{L}^{em}_{quarks} = \bar{\psi}\left(i\gamma^\mu\partial_\mu - m + \hat{\mu}\gamma^0 + \tilde{e}\gamma^\mu\tilde{A}_\mu\tilde{Q}\right)\psi, \tag{2.1}$$

where $\tilde{A}_\mu$ is the rotated massless $\tilde{U}(1)_{em}$ gauge field. This field is a linear combination of the vacuum photon A_μ and the 8th gluon A^8_μ as we discussed in Sec. 1.5. The quarks carry flavor and color indices ψ_{ia}, where $i \in (u,d) = (1,2)$ is the flavor

index and $a \in (r,g,b) = (1,2,3)$ is the color index. The multi-component quark spinor field ψ is assumed to have the following explicit form:

$$\psi = \begin{pmatrix} \psi_{ur} \\ \psi_{ug} \\ \psi_{ub} \\ \psi_{dr} \\ \psi_{dg} \\ \psi_{db} \end{pmatrix}. \tag{2.2}$$

Here we assume that up and down quarks have the same masses ($m_u = m_d = m$). In the 2SC phase, the matrix of chemical potentials $\hat{\mu}$ can have a nontrivial color-flavor structure. When β-equilibrium and neutrality of quark matter is imposed [93, 94], the matrix elements of $\hat{\mu}$ read

$$\mu_{ij,ab} = [\mu\,\delta_{ij} - \mu_e (Q_f)_{ij}]\,\delta_{ab} + \frac{2}{\sqrt{3}}\mu_8 \delta_{ij} (T_8)_{ab}, \tag{2.3}$$

where only one out of three parameters (μ, μ_e and μ_8) is truly independent, while the other two must be adjusted to achieve color and electric neutrality. For subtleties regarding the color neutrality, see Ref. [123].

The explicit form of the quasiparticle charge operator $\tilde{Q}$, that corresponds to $\tilde{U}(1)_{em}$ gauge group, has been discussed in Sec. 1.5 and given by Eq. (1.12). In units of $\tilde{e} = eg/\sqrt{g^2 + e^2/3}$, the $\tilde{Q}$ charges of quarks are given in Table 1.2 (p.16).

In order to simplify the explicit form of the quark propagators in the magnetic 2SC phase, it is convenient to introduce the following set of projectors onto the subspaces of quasiparticles with different values of rotated-charges [117, 118]:

$$\Omega_{+\frac{1}{2}} = \mathsf{diag}(1,1,0,0,0,0), \tag{2.4}$$

$$\Omega_{+1} = \mathsf{diag}(0,0,1,0,0,0), \tag{2.5}$$

$$\Omega_{-\frac{1}{2}} = \mathsf{diag}(0,0,0,1,1,0), \tag{2.6}$$

$$\Omega_{0} = \mathsf{diag}(0,0,0,0,0,1). \tag{2.7}$$

This is a complete set of projectors, satisfying the following relations:

$$\Omega_{\tilde{Q}}\Omega_{\tilde{Q}'} = \delta_{\tilde{Q}\tilde{Q}'}\Omega_{\tilde{Q}}, \qquad \tilde{Q},\tilde{Q}' = \pm 1/2, +1, 0. \tag{2.8}$$

$$\Omega_{+\frac{1}{2}} + \Omega_{+1} + \Omega_{-\frac{1}{2}} + \Omega_0 = 1. \tag{2.9}$$

By making use of these projectors, we can decompose the multi-component quark spinor field into separate pieces, describing groups of quasiparticles with different rotated charges:

$$\psi = \psi_{(+\frac{1}{2})} + \psi_{(+1)} + \psi_{(-\frac{1}{2})} + \psi_{(0)}, \tag{2.10}$$

where, by definition,

$$\psi_{(+\frac{1}{2})} = \Omega_{+\frac{1}{2}}\psi, \qquad \psi_{(+1)} = \Omega_{+1}\psi, \qquad \psi_{(-\frac{1}{2})} = \Omega_{-\frac{1}{2}}\psi, \qquad \psi_{(0)} = \Omega_0\psi. \tag{2.11}$$

In the new notation, the quadratic part of the quark Lagrangian density can be rewritten as follows:

$$\mathcal{L}^{em}_{quarks} = \sum_{\tilde{Q}=\pm 1/2,+1,0} \bar{\psi}_{(\tilde{Q})}(i\gamma^\mu\partial_\mu - m + \mu_{\tilde{Q}}\gamma^0 + \tilde{e}\tilde{Q}\gamma^\mu\tilde{A}_\mu)\psi_{(\tilde{Q})}. \tag{2.12}$$

As follows from Eq. (2.3), the chemical potentials $\mu_{\tilde{Q}}$ for quasiparticles with different $\tilde{Q}$-charges, when projected onto the relevant color-flavor subspaces, are given by

$$\mu_{(+\frac{1}{2})} = \mu_{ur} = \mu_{ug} = \mu - \frac{2}{3}\mu_e + \frac{1}{3}\mu_8, \tag{2.13}$$

$$\mu_{(-\frac{1}{2})} = \mu_{dr} = \mu_{dg} = \mu + \frac{1}{3}\mu_e + \frac{1}{3}\mu_8, \tag{2.14}$$

$$\mu_{(+1)} = \mu_{ub} = \mu - \frac{2}{3}\mu_e - \frac{2}{3}\mu_8, \tag{2.15}$$

$$\mu_{(0)} = \mu_{db} = \mu + \frac{1}{3}\mu_e - \frac{2}{3}\mu_8. \tag{2.16}$$

In this study, in order to simplify the analysis of the gap equation we will eventually neglect the effects due to nonzero μ_e and μ_8. This is certainly justified in the study of QCD at asymptotically large densities. On the other hand, if the analysis is to be extrapolated to moderately large densities, relevant for compact stars, nonvanishing μ_e and μ_8 may become important [93, 94, 95, 124, 125, 126, 127, 128, 129,

130, 131]. One should keep in mind, however, that the study of such a moderate-density quark matter from first principles will be still quantitatively unreliable within the framework of the Schwinger-Dyson equation because of the strong-coupling regime. As for the main purpose of this study, it aims only at a better understanding of the qualitative role of long-range forces.

2.3 Quasiparticle Propagators

In the 2SC color-superconducting phase, only the quasiparticles with the charges $\tilde{Q} = \pm\frac{1}{2}$ participate in Cooper pairing, while the remaining two quasiparticles (with charges $\tilde{Q} = 0, 1$) play the role of passive spectators. Therefore, in the rest of the analysis, we will concentrate exclusively on the two pairs of quasiparticles participating in Cooper pairing and ignore the others.

As usual in studies of color-superconducting phases, it is convenient to introduce the Nambu-Gorkov spinors,

$$\bar{\Psi}_{(\tilde{Q})} = (\bar{\psi}_{(\tilde{Q})}, \bar{\psi}^{C}_{(-\tilde{Q})}), \qquad \Psi_{(\tilde{Q})} = \begin{pmatrix} \psi_{(\tilde{Q})} \\ \psi^{C}_{(-\tilde{Q})} \end{pmatrix}, \tag{2.17}$$

for quasiparticles with the charges $\tilde{Q} = \pm\frac{1}{2}$. Here $\psi^{C}_{(\tilde{Q})} = C\bar{\psi}^{T}_{(\tilde{Q})}$ and $\bar{\psi}^{C}_{(\tilde{Q})} = \psi^{T}_{(\tilde{Q})}C$ are the charge-conjugate spinors, and $C = i\gamma^2\gamma^0$ is the charge-conjugation matrix satisfying the relations: $C^{-1}\gamma^{\mu}C = -(\gamma^{\mu})^{T}$ and $C = -C^{T}$. In terms of the Nambu-Gorkov spinors, Lagrangian density (2.12) takes the form

$$\mathcal{L}^{em}_{quarks} = \frac{1}{2}\sum_{\tilde{Q}=\pm 1/2} \bar{\Psi}_{(\tilde{Q})} S^{-1}_{(\tilde{Q}),0} \Psi_{(\tilde{Q})} + \sum_{\tilde{Q}=+1,0} \bar{\psi}_{(\tilde{Q})} [G^{+}_{(\tilde{Q}),0}]^{-1} \psi_{(\tilde{Q})}, \tag{2.18}$$

where the inverse free propagator $S^{-1}_{(\tilde{Q}),0}$ for each sector with a fixed value of $\tilde{Q}$-charge has a block-diagonal form,

$$S^{-1}_{(\tilde{Q}),0} = \mathrm{diag}\left([G^{+}_{(\tilde{Q}),0}]^{-1}, [G^{-}_{(\tilde{Q}),0}]^{-1} \right), \tag{2.19}$$

and the explicit form of the diagonal elements reads

$$\left[G^{\pm}_{(\tilde{Q}),0}\right]^{-1} = \gamma^{\mu}\left(i\partial_{\mu} + \tilde{Q}\tilde{e}\tilde{A}_{\mu}\right) \pm \mu_{(\tilde{Q})}\gamma^{0} - m. \tag{2.20}$$

For quasiparticles participating in Cooper pairing, the full propagators also have nonzero off-diagonal Nambu-Gorkov components, determined by the color-superconducting gap function, i.e.,

$$S^{-1}_{(\tilde{Q})} = \begin{pmatrix} [G^{+}_{(\tilde{Q}),0}]^{-1} & \Delta^{-}_{(\tilde{Q})} \\ \Delta^{+}_{(\tilde{Q})} & [G^{-}_{(\tilde{Q}),0}]^{-1} \end{pmatrix}. \tag{2.21}$$

The color-flavor structures of $\Delta^{-}_{(\tilde{Q})}$ and $\Delta^{+}_{(\tilde{Q})}$ are given by

$$\Delta^{-}_{(+\frac{1}{2})} = -\Delta^{-}_{(-\frac{1}{2})} = \begin{pmatrix} 0 & -i\gamma^{5}\Delta \\ i\gamma^{5}\Delta & 0 \end{pmatrix}, \tag{2.22}$$

$$\Delta^{+}_{(+\frac{1}{2})} = -\Delta^{+}_{(-\frac{1}{2})} = \begin{pmatrix} 0 & i\gamma^{5}\Delta^{*} \\ -i\gamma^{5}\Delta^{*} & 0 \end{pmatrix}. \tag{2.23}$$

Note that the explicit forms of the two relevant Nambu-Gorkov spinors (A.1) read

$$\Psi_{(+\frac{1}{2})} = \begin{pmatrix} \psi_{ur} \\ \psi_{ug} \\ \psi^{C}_{dr} \\ \psi^{C}_{dg} \end{pmatrix}, \qquad \Psi_{(-\frac{1}{2})} = \begin{pmatrix} \psi_{dr} \\ \psi_{dg} \\ \psi^{C}_{ur} \\ \psi^{C}_{ug} \end{pmatrix}. \tag{2.24}$$

It appears that one can partially diagonalize the inverse full propagators $S^{-1}_{(\tilde{Q})}$ by simply reordering the components of the spinors as follows:

$$\Psi^{new}_{(+\frac{1}{2})} = \begin{pmatrix} \psi_{ur} \\ \psi^{C}_{dg} \\ \psi_{ug} \\ \psi^{C}_{dr} \end{pmatrix}, \qquad \Psi^{new}_{(-\frac{1}{2})} = \begin{pmatrix} \psi_{dr} \\ \psi^{C}_{ug} \\ \psi_{dg} \\ \psi^{C}_{ur} \end{pmatrix}. \tag{2.25}$$

From physics viewpoint, the possibility of such a partial diagonalization reflects the fact that there are two different types of Cooper pairs: one made of red up and green down quarks and the other made of green up and red down quarks.

In the new basis, the inverse full propagator $S^{-1}_{(\tilde{Q})}$ has the following block-diagonal form:

$$S^{-1}_{(\tilde{Q})} = \text{diag}\left([S^X_{(\tilde{Q})}]^{-1}, [S^Y_{(\tilde{Q})}]^{-1}\right), \tag{2.26}$$

where

$$[S^X_{(+\frac{1}{2})}]^{-1} = \begin{pmatrix} \gamma^\mu(i\partial_\mu + \frac{1}{2}\tilde{e}\tilde{A}_\mu) + \mu_{ur}\gamma^0 - m & -i\gamma^5\Delta \\ -i\gamma^5\Delta^* & \gamma^\mu(i\partial_\mu + \frac{1}{2}\tilde{e}\tilde{A}_\mu) - \mu_{dg}\gamma^0 - m \end{pmatrix}, \tag{2.27}$$

$$[S^Y_{(+\frac{1}{2})}]^{-1} = \begin{pmatrix} \gamma^\mu(i\partial_\mu + \frac{1}{2}\tilde{e}\tilde{A}_\mu) + \mu_{ug}\gamma^0 - m & i\gamma^5\Delta \\ i\gamma^5\Delta^* & \gamma^\mu(i\partial_\mu + \frac{1}{2}\tilde{e}\tilde{A}_\mu) - \mu_{dr}\gamma^0 - m \end{pmatrix}, \tag{2.28}$$

and

$$[S^X_{(-\frac{1}{2})}]^{-1} = \begin{pmatrix} \gamma^\mu(i\partial_\mu - \frac{1}{2}\tilde{e}\tilde{A}_\mu) + \mu_{dr}\gamma^0 - m & i\gamma^5\Delta \\ i\gamma^5\Delta^* & \gamma^\mu(i\partial_\mu - \frac{1}{2}\tilde{e}\tilde{A}_\mu) - \mu_{ug}\gamma^0 - m \end{pmatrix}, \tag{2.29}$$

$$[S^Y_{(-\frac{1}{2})}]^{-1} = \begin{pmatrix} \gamma^\mu(i\partial_\mu - \frac{1}{2}\tilde{e}\tilde{A}_\mu) + \mu_{dg}\gamma^0 - m & -i\gamma^5\Delta \\ -i\gamma^5\Delta^* & \gamma^\mu(i\partial_\mu - \frac{1}{2}\tilde{e}\tilde{A}_\mu) - \mu_{ur}\gamma^0 - m \end{pmatrix}. \tag{2.30}$$

Using the representation for the inverse quasiparticle propagator in Eq. (2.26), we find the propagator itself,

$$S_{(\tilde{Q})} = \text{diag}\left(S^X_{(\tilde{Q})}, S^Y_{(\tilde{Q})}\right). \tag{2.31}$$

The calculation of the corresponding diagonal blocks $S^{X,Y}_{(\tilde{Q})}$ is tedious, but straightforward. The details of derivation are presented in Appendix B.

2.4 Gap Equation

In the coordinate space, the gap equation (i.e., the off-diagonal component of the Schwinger-Dyson equation for the full propagator) reads

$$\left[S^X_{(\tilde{Q})}\right]^{-1}_{21}(u,u') = ig^2\gamma^\mu\left(-T^A\right)^T\left[S^X_{(\tilde{Q})}\right]_{21}(u,u')\gamma^\nu T^B D^{AB}_{\mu\nu}(u,u'), \tag{2.32}$$

where $D_{\mu\nu}(u,u')$ is the gluon propagator, and $u \equiv (t,z,\boldsymbol{r}_\perp)$ is a four-vector of space-time position. We will assume that the gluon propagator is diagonal in adjoint color indices. Note that the off-diagonal component of the propagator $S^Y_{(\tilde{Q})}$ satisfies a similar equation. While Eq. (2.32) describes Cooper pairing of red up and green down quarks, the equation for $S^Y_{(\tilde{Q})}$ describes Cooper pairing of green up and red down quarks.

In this study of Cooper pairing in a magnetized color-superconducting phase, it is convenient to start from the coordinate-space representation of the gap equation, see Eq. (2.32), and then switch to the Landau-level representation. This is in contrast to the usual momentum-space representation, often utilized in the case of vanishing external fields.

In this connection, a short remark is in order regarding the general structure of a quasiparticle propagator. Because of the interaction of charged quasiparticles with the magnetic field, their momenta in the two spatial directions perpendicular to the field are not well defined quantum numbers. This is reflected in the structure of the propagator (as well as its inverse), which is not a translationally invariant function in coordinate space. Instead, the quasiparticle propagator has the form of a product of the universal Schwinger phase (which spoils the translational invariance) and a translationally invariant part [132] (for details, see Appendix B.)

After factoring out the same Schwinger phase on both sides of the gap equation and projecting the resulting equation onto subspaces of different Landau levels, one obtains an infinite set of coupled equations, see Eq. (C.6) in Appendix C. For both charges $\tilde{Q} = \pm 1/2$, the gap equations are similar. Here we show only the final set of equations for $\tilde{Q} = +1/2$:

$$\begin{aligned}\Delta_m \mathcal{P}_- + \Delta_{m+1}\mathcal{P}_+ &= -i\frac{2g^2}{3}\sum_{n=0}^{\infty}\int\frac{d\omega' dk'^3}{(2\pi)^2}\int\frac{d^2\boldsymbol{q}_\perp}{(2\pi)^2}\gamma^\mu\frac{\Delta_n\mathcal{E}_n}{\mathcal{C}_n}\left[\mathcal{L}^{(0)}_{n,m}\left(\frac{q_\perp^2 l^2}{2}\right)\mathcal{P}_-\right. \\ &\left. +\mathcal{L}^{(0)}_{n-1,m}\left(\frac{q_\perp^2 l^2}{2}\right)\mathcal{P}_+\right]\gamma^\nu D_{\mu\nu}(\omega-\omega', k^3-k'^3, \boldsymbol{q}_\perp), \quad (2.33)\end{aligned}$$

where $m, n = 0, 1, 2, \ldots$ are Landau-level indices, and functions $\mathcal{C}_n$ and $\mathcal{E}_n$ are defined in Appendix B, see Eq. (B.16) and (B.20), respectively. These functions depend on the parameters of the model (e.g., masses and chemical potentials of quarks) as well as on the color-superconducting gap parameters Δ_n. Note that the gaps associated with different Landau levels are not necessarily equal. This fact is emphasized by the Landau-level subscript n in the notation. Here and below, we assume that all gaps Δ_n are real functions.

Gluon Propagator

In dense quark matter, unlike in vacuum, the gluon exchange interaction is partially screened. Therefore, when analyzing the Cooper pairing dynamics between quarks, it is very important to take the relevant screening effects due to nonzero density into consideration [56]. In the problem at hand, in addition, one should account for the external magnetic field, which can further modify the screening of the one-gluon interaction through quark loops. The latter can be quite important in strong magnetic fields [133]. To simplify the analysis in this study, we will assume that the magnetic field is weak ($|eB| \ll \mu^2$). At the end, we shall see that this happens to be a very good approximation for most stellar applications.

In the case of a weak external field, the screening of the one-gluon interaction in dense medium can be described well by the usual hard-dense loop approximation [134, 135, 136]. In the Coulomb gauge, the Lorentz structure of the gluon propagator is given by [137, 138]

$$D_{\mu\nu}(Q) = -\frac{Q^2}{q^2}\frac{\delta_{\mu 0}\delta_{\nu 0}}{Q^2 - F} - \frac{P^T_{\mu\nu}}{Q^2 - G}, \tag{2.34}$$

where functions F and G define the spectra of the longitudinal and transverse gluons, respectively. Both functions depend on the energy q^0 and the absolute value of the three-momentum $|\vec{q}|$. By definition, $Q = (q^0, \vec{q})$ is a momentum four-vector. The transverse Lorentz projector $P^T_{\mu\nu}$ is defined as follows:

$$P^T_{00} = P^T_{0i} = 0, \qquad P^T_{ij} = \delta_{ij} - \hat{q}_i\hat{q}_j. \tag{2.35}$$

In the most important regime for Cooper pairing dynamics, $q^0 \ll |\vec{q}| \ll m_D$, the approximate expressions for these screening functions read [134, 135, 136]

$$F \simeq m_D^2, \qquad G \simeq \frac{\pi}{4} m_D^2 \frac{q^0}{|\vec{q}|}, \tag{2.36}$$

where $m_D^2 = (g\mu/\pi)^2$ is the Debye screening mass in two-flavor quark matter. At large densities, the exchange interaction by electric gluon modes is strongly suppressed due to Debye screening and, to leading order, plays no role. Magnetic gluon modes, on the other hand, are subject only to a mild dynamical screening (Landau damping) at nonzero frequencies and play the dominant role in Cooper pairing [56].

Gap Equation: Weak Magnetic Field Limit

In order to obtain the gap equation in the weak magnetic field limit, we expand the translationally invariant part of the full fermion propagator in powers of the magnetic field and keep the leading terms up to second order, $(\tilde{e}\tilde{Q}\tilde{B})^2$ (for details, see Appendix D and E. Omitting the technical details, here we present the final form of the

gap equation,

$$\Delta(\omega) = T^{(0)}(\omega) + T^{(1)}(\omega) + T^{(2)}(\omega), \tag{2.37}$$

where

$$T^{(i)}(\omega) = -i\frac{2g^2}{3}\int\frac{d\omega'}{2\pi}\int\frac{d^3\boldsymbol{k}'}{(2\pi)^3}\Delta(\omega')\gamma^\mu K^{(i)}(\omega',\boldsymbol{k}')\gamma^\nu D_{\mu\nu}(\omega-\omega',\boldsymbol{k}-\boldsymbol{k}') \tag{2.38}$$

is the contribution of the ith order in powers of the magnetic field. The explicit form of the kernels $K^{(i)}(\omega,\boldsymbol{k})$ for the three leading-order terms in the gap equation are presented in Eqs. (D.22), (D.23) and (D.24) in Appendix D.

At zero magnetic field, Eq. (2.37) reduces to the well known gap equation in the 2SC phase without a magnetic field [56, 57, 58, 59, 60, 61, 62, 63, 64, 139, 140]. After switching to Euclidean space and performing the traces on both sides of the gap equation, we rederive the following 0th order (i.e., vanishing magnetic field) equation:

$$\begin{aligned}\Delta^{(0)}(\omega_E) &= \frac{g^2}{3}\int\frac{d\omega'_E}{(2\pi)}\int\frac{d^3\boldsymbol{k}'}{(2\pi)^3}\frac{\Delta^{(0)}(\omega'_E)}{(\omega'_E)^2+(k'-\bar{\mu})^2+[\Delta^{(0)}(\omega'_E)]^2}\\ &\quad\times\left[\frac{1}{(\omega_E-\omega'_E)^2+|\boldsymbol{k}-\boldsymbol{k}'|^2+m_D^2}+\frac{2|\boldsymbol{k}-\boldsymbol{k}'|}{|\boldsymbol{k}-\boldsymbol{k}'|^3+\omega_l^3}\right],\end{aligned} \tag{2.39}$$

where $k=|\boldsymbol{k}|$, $k'=|\boldsymbol{k}'|$, $\omega_E=i\omega$, $\omega'_E=i\omega'$ and $\omega_l^3=(\pi/4)m_D^2|\omega'_E-\omega_E|$. For simplicity, here we assumed that $m=0$ and that the chemical potentials of all quarks are identical and equal to $\bar{\mu}$.

After performing the integration over $\boldsymbol{k}'$ and keeping only the leading-order contributions from the dynamically-screened magnetic gluon exchange, we arrive at

$$\Delta^{(0)}(\omega_E) = \frac{g^2}{36\pi^2}\int_{-\infty}^{\infty}d\omega'_E\frac{\Delta^{(0)}(\omega'_E)}{\sqrt{(\omega'_E)^2+(\Delta^{(0)})^2}}\ln\frac{\Lambda}{|\omega'_E-\omega_E|}, \tag{2.40}$$

where $\Lambda=4(2\mu)^3/(\pi m_D^2)$. The approximate solution to this equation reads [56, 57, 58, 59, 60, 61, 62, 63, 64, 139, 140]

$$\Delta^{(0)}\simeq\Lambda\exp(-\frac{3\pi^2}{\sqrt{2}g}+1). \tag{2.41}$$

For completeness of the presentation, the derivation of this result is reviewed in Appendix A. Using this result as a benchmark, let us proceed to the case of a weak but nonzero magnetic field.

It is easy to check (and might have been expected from the symmetry arguments) that the first order term, i.e., $T^{(1)}(\omega)$ in Eq. (2.38), which is linear in a magnetic field, vanishes after the Dirac traces are performed. Thus, the leading correction to the gap equation in a weak magnetic field comes from the second order term, i.e., $T^{(2)}(\omega)$ in Eq. (2.38).

To the same leading order in coupling, which includes only the exchange interaction due to dynamically-screened magnetic gluons, we derive the following explicit form of the gap equation (for the details of derivation, see Appendix E) :

$$\Delta^{(B)}(\omega_E) = \frac{g^2}{36\pi^2}\int_{-\infty}^{\infty} d\omega'_E \Delta^{(B)}(\omega'_E)\left[\frac{1}{\sqrt{(\omega'_E)^2+(\Delta^{(B)})^2}}\ln\frac{\Lambda}{|\omega'_E-\omega_E|}+\right.$$
$$\left.+\frac{9\omega_l^{15}(\tilde{e}\tilde{Q}\tilde{B})^2\sin^2\theta_{Bk}}{4\bar{\mu}^2\left(\omega_l^6+[(\omega'_E)^2+(\Delta^{(B)})^2]^3\right)}\ln\frac{\omega_l}{|\omega'_E-\omega_E|}\right]. \quad (2.42)$$

The detailed analysis of this equation may not be very easy. However, several of its qualitative properties are obvious right away. First of all, the positive sign of the subleading order correction, proportional to $(\tilde{e}\tilde{Q}\tilde{B})^2$, indicates that the gap increases with the magnetic field. This is in qualitative agreement with the intuitive expectation that the external magnetic field should enhance the binding energy of Cooper pairs made of quasiparticles with opposite charges [112, 113, 114, 115, 116, 117, 118]. From the fact that this correction to the gap equation is also proportional to $\sin^2\theta_{Bk}$, where θ_{Bk} is the angle between the quasiparticle momentum and the magnetic field, we conclude that the gap function acquires a directional dependence. Moreover, we see that the largest value of the gap will be for quasiparticles with the momenta perpendicular to the magnetic field. On the other hand, for quasiparticles with the momenta parallel to the field, there is no enhancement of the gap at all.

In order to understand the qualitative effect of the subleading term quadratic in magnetic field, we can perform the following semi-rigorous analysis of Eq. (2.42). To this end, let us cut the infrared region of integration off at $\omega_E' = \Delta^{(B)}$ and substitute $\Delta^{(B)} = 0$ in the denominators of both terms on the right-hand side of the equation. We then arrive at

$$\Delta^{(B)} \simeq \frac{g^2}{18\pi^2}\left(1+\frac{54\pi(\tilde{e}\tilde{Q}\tilde{B})^2}{g^2\bar{\mu}^4}\sin^2\theta_{Bk}\right)\int_{\Delta^{(B)}}^{\Lambda} d\omega_E' \frac{\Delta^{(B)}}{\omega_E'}\ln\frac{\Lambda}{\omega_E'}. \tag{2.43}$$

While this approximation cannot be used to get a reliable estimate for the gap, it is very helpful to understand the qualitative effect of the magnetic field on the pairing dynamics in color-superconducting dense quark matter. It shows that the effective coupling constant in the presence of a magnetic field becomes larger, i.e.,

$$g^2 \to g_{eff}^2 = g^2\left(1+\frac{27\pi(\tilde{e}\tilde{B})^2}{2g^2\bar{\mu}^4}\sin^2\theta_{Bk}\right), \tag{2.44}$$

where we substituted $\tilde{Q} = \pm\frac{1}{2}$. The validity of the weak-field approximation requires that the subleading correction is small compared to the leading result. This translates into the requirement $|\tilde{e}\tilde{B}|^2 \lesssim g^2\bar{\mu}^4$. As we shall see below, this condition is always satisfied in stellar applications.

Without rigorously solving the gap equation (2.42), now we can claim that the solution for the gap function in the magnetic 2SC phase is approximately given by the same expression as in the absence of the field, but with the coupling constant g replaced by g_{eff}, i.e.,

$$\Delta^{(B)} \simeq \Lambda\exp(-\frac{3\pi^2}{\sqrt{2}g_{eff}}+1) \simeq \Delta^{(0)}e^{\beta_{Bk}}, \tag{2.45}$$

where the explicit expression for β_{Bk} follows from Eq. (2.44),

$$\beta_{Bk} = \frac{81\pi^3(\tilde{e}\tilde{B})^2}{4\sqrt{2}g^3\bar{\mu}^4}\sin^2\theta_{Bk}. \tag{2.46}$$

This is a nonnegative function, which depends on the angle between the quasiparticle momentum $\boldsymbol{k}$ and the magnetic field $\tilde{\boldsymbol{B}}$. The maximum value $\beta_{Bk}^{(max)}$ is obtained $\theta_{Bk} = 90^{\circ}$

The final result in Eq. (2.45) is interesting for several reasons. Most importantly, it shows that the gap is non-isotropic, taking its largest values when the quasiparticle momenta are perpendicular to the direction of the magnetic field, and taking its smallest value when the quasiparticle momenta are along/against the field. We also find that, compared to the case without the magnetic field, the gap is subject to an increase in all directions of quasiparticle momenta, except for the directions exactly along or against the magnetic field.

Gap Equation: Strong Magnetic Field Limit

To get a qualitative insight about the pairing dynamics in the case of a strong magnetic field, $\tilde{e}\tilde{B} \gtrsim \mu^2$, it seems sufficient to consider the gap equation in the lowest Landau-level approximation. The choice of a simple approximation for the gluon exchange interaction is much harder to justify. Here we will use the gluon propagator with the screening effects at zero magnetic field. Obviously, such an approximation is not very reliable. A naive justification for such an approximation is the observation that gluons couple not only to the charged quasiparticles (with $\tilde{Q} = \pm 1/2$ and $\tilde{Q} = 1$), which are strongly affected by the magnetic field, but also to neutral quasiparticles (with $\tilde{Q} = 0$), which are not affected by the magnetic field at all. If the zero-density ($\mu = 0$) and strong-magnetic field limit in gauge theories is used as a guide for intuition, one may suggest that those gluons, which are coupled only to charged quasiparticles, will be subject to an additional Debye screening with an effective mass $m_D^{eff} \propto g\sqrt{|\tilde{e}\tilde{B}|}$ [133]. The other gluons will be still providing the same dominant interaction with dynamical screening as in absence of the exter-

nal field. Then, the usual hard-dense-loop approximation may be still qualitatively reasonable. Besides, to the best of our knowledge, the explicit result for the polarization tensor (screening) in dense QCD matter ($\mu \neq 0$) in a magnetic field ($B \neq 0$) is not available in the literature. Thus, the main purpose of our exercise in this subsection, which is based on the simplest possible approximation, will be to roughly estimate the color-superconducting gap due to long-range interaction in the regime of a strong external magnetic field.

By making use of Eq. (2.33), we easily derive the gap equation in the lowest Landau-level approximation,

$$\begin{aligned}\Delta^{(B)}(\omega_E) &= \frac{g^2}{3}\int\frac{d\omega_E' dk'^3}{(2\pi)^2}\int\frac{d^2\boldsymbol{q}_\perp}{(2\pi)^2}\exp\left(-\frac{q_\perp^2 l^2}{2}\right)\frac{\Delta^{(B)}(\omega_E')}{(\omega_E')^2+(k'^3-\mu)^2+(\Delta^{(B)})^2} \\ &\times\frac{q_\perp^2}{(k'^3-k^3)^2+q_\perp^2}\frac{[(k'^3-k^3)^2+q_\perp^2]^{\frac{1}{2}}}{[(k'^3-k^3)^2+q_\perp^2]^{\frac{3}{2}}+\omega_l^3}. \end{aligned} \tag{2.47}$$

Because of the exponential suppression in the integration over the transverse momentum $q_\perp$, the dominant contribution comes from the region of small momenta, $q_\perp l \lesssim 1$. Therefore, an approximate result can be obtained by simply making a sharp ultraviolet cutoff at $q_\perp = \sqrt{2}/l$ and dropping altogether the exponential factor $\exp(-q_\perp^2 l^2/2)$ in the integrand. After performing the integration also over the longitudinal momentum k'^3, we will arrive at the following approximate gap equation:

$$\Delta^{(B)}(\omega_E) \approx \frac{g^2}{72\pi^2}\int_{-\infty}^{+\infty} d\omega_E'\frac{\Delta^{(B)}(\omega_E')}{\sqrt{(\omega_E')^2+(\Delta^{(B)})^2}}\ln\frac{\Lambda_B}{|\omega_E'-\omega_E|}, \tag{2.48}$$

where $\Lambda_B = \frac{8\sqrt{2}}{\pi m_D^2 l^3} = \frac{8\pi\sqrt{2}|\tilde{e}\tilde{Q}\tilde{B}|^{3/2}}{g^2\bar{\mu}^2}$. As we see, this equation has the same structure as Eq. (2.40), but with a smaller effective coupling and a different expression for Λ_B. Making use of this fact, we can get an approximate solution for the gap in the limit of strong magnetic field by properly modifying the result in Eq. (2.41), i.e.,

$$\Delta^{(B)} = \frac{4\pi|\tilde{e}\tilde{B}|^{3/2}}{g^2\bar{\mu}^2}\exp(-\frac{3\pi^2}{g}+1). \tag{2.49}$$

Here we substituted $\tilde{Q} = \pm\frac{1}{2}$. This result shows that the strong magnetic field strengthens the diquark pair formation. This is in qualitative agreement with the findings in models with local interaction [112, 113, 114, 115, 116, 117, 118].

In contrast to the result in the weak-magnetic field limit, there is no directional dependence in the gap function when the field is strong. This suggests that the corresponding pairing dynamics is essentially local. While the result may appear surprising at first sight, this finding in fact agrees with the intuitive picture that the motion of charged particles is restricted over distances of the order of the magnetic length, $l = 1/\sqrt{|\tilde{e}\tilde{Q}\tilde{B}|}$, in the plane perpendicular to the magnetic field. When Cooper pairs form, the additional spatial restriction on particles' motion (partial localization) can strongly enhance the binding energy and substantially reduce the size of bound states.

CHAPTER 3

SUMMARY & OUTLOOK

In Chapter 1, we reviewed a schematic phase diagram for QCD. It has been argued that cold and dense quark matter is expected to be a color superconductor. Such matter may exist in the interiors of neutron stars. The two simplest spin-zero color superconductors, the CFL and 2SC phases, can be realized by applying the BCS mechanism to a many-quark system at sufficiently low temperatures and high densities. The symmetry properties of the CFL and 2SC phases are discussed in detail by analyzing the color-flavor structure of the Cooper pairing patterns in these two phases. For both phases, the magnitude of the gap parameters can be investigated perturbatively by making use of the Schwinger-Dyson equation in the weak-coupling limit of QCD. These are the examples of very few reliable calculations of non-perturbative quantities in QCD, which are obtained from first principles. In addition, some other features, including charge neutrality, beta equilibrium and strange quark mass, are also discussed in general. Note that a mismatch of the Fermi momenta of different quark flavors arises because of them and could complicate the formation of diquark Cooper pairs. It is of great significance to make a theoretical analysis of color superconductivity. Starting from the derivations and calculations of the properties (e.g., equation of state, neutrino emissivity and conductivities) for different color superconductors by using QCD theory or other effective models, we can find how they affect the physical phenomena and observables of neutron stars. And then comparing with astrophysical data from experimental measurement, we can clarify the occurrence of different forms of quark matter in the central region of neutron stars and deepen our understanding of the behavior of dense quark matter.

In the main part of this thesis, we studied the effect of a “rotated” magnetic field on the Cooper pairing dynamics in the two-flavor color-superconducting phase

of dense quark matter with a long-range interaction provided by the one-gluon exchange with dynamical screening. Using the Landau-level representation, we derived a set of gap equations valid for an arbitrary magnetic filed. These equations show that, in general, the gaps are functions of the Landau-level index n. Therefore, solving the corresponding set of equations may be rather involved and require the use of sophisticated numerical methods. Instead, here we used analytical methods to investigate the limiting cases of weak and strong magnetic fields [122].

In the weak-magnetic field limit, the energy separation between the Landau levels is vanishingly small and there is no reason to expect a strong dependence of the gaps on the corresponding discrete index n. This justifies the use of an approximation in which the gaps are the same in all Landau levels near the Fermi surface. Additionally, in this case the quasiparticle propagator allows a simple expansion in powers of the magnetic field that greatly simplifies the structure of the resulting gap equation, see Eq. (2.37). We find that the leading-order term affecting the gap, is quadratic in the magnetic field. The corresponding correction to the vanishing magnetic field result for the gap is determined by the value of parameter $\beta_{Bk}^{(max)} = 81\pi^3(\tilde{e}\tilde{B})^2/(4\sqrt{2}g^3\bar{\mu}^4)$, where $\tilde{B}$ is the magnetic field and $\bar{\mu}$ is the quark chemical potential, see Eq. (2.46). The numerical value of this parameter appears to be quite small even for strongest possible magnetic fields in compact stars, $\tilde{B} \lesssim 10^{18}$ G. Indeed, the corresponding numerical estimate reads

$$\beta_{Bk}^{(max)} \approx 1.3 \times 10^{-2} \left(\frac{400 \text{ MeV}}{\bar{\mu}}\right)^4 \left(\frac{\tilde{B}}{10^{18} \text{ G}}\right)^2 . \tag{3.1}$$

(Here, for the strong coupling constant, we used $g = \sqrt{4\pi}$, which corresponds to $\alpha_s = 1$.)

The most interesting feature of the pairing dynamics in the presence of a magnetic field is a directional dependence of the gap function in momentum space.

The magnetic field correction to the gap is proportional to $\sin^2\theta_{Bk}$, where θ_{Bk} is the angle between the quasiparticle momentum $\boldsymbol{k}$ and the magnetic field $\tilde{\boldsymbol{B}}$. From a physics viewpoint, this means that quasiparticles with momenta pointing perpendicular to the direction of the magnetic field have the largest gaps, while quasiparticles with momenta along/against the field have the smallest gaps. Clearly, such a directional dependence is a qualitative outcome of a long-range interaction in the model used. This contrasts with the studies based on models with point-like interactions in Refs. [112, 113, 114, 115, 116, 117, 118], where the gaps are always isotropic.

Our analysis in the case of a strong magnetic field is admittedly less rigorous. We use the lowest Landau-level approximation and utilize the simplest approximation for the gluon exchange interaction without modifying the screening effects due to a nonzero magnetic field. The resulting estimate for the gap is given in Eq. (2.49). Our result shows that strong magnetic fields enhance the diquark Cooper pairing and lead to larger color-superconducting gaps. This is in qualitative agreement with the findings in Refs. [112, 113, 114, 115, 116, 117, 118], where models with short-range interactions were used. We also find that, because of the partial localization of quasiparticles in a strong magnetic field, the corresponding dynamics is essentially local and there is no directional dependence of the gap.

To go beyond the two limiting cases analyzed in this thesis, one will need to properly truncate an infinite set of gap equations and use numerical methods to solve it. In such an approach, it may be also possible to include the effects of different quark masses and chemical potentials. The corresponding study, when extrapolated to the regime of realistic densities, may further extend our understanding of dense quark matter by clarifying (i) possible directional dependences of the gap function, (ii) the evolution of such a dependence between the two limiting cases

studied here, and (iii) the effect of β-equilibrium and neutrality of quark matter on the gap function in magnetic fields. All of these topics are left for future investigations.

Additionally, it is of great interest to address how external magnetic fields affect the properties of the neutron stars, such as the equation of state, neutrino emissivity, specific heat, thermal conductivities, and viscosities, which have been discussed in Sec. 1.7. The possible astrophysical consequences can help to search for observational signatures, to shed some light on the existence of color superconductivity, and perhaps, to distinguish between different color-superconducting phases.

REFERENCES

[1] C. N. Yang and R. L. Mills, "Conservation of isotopic spin and isotopic gauge invariance," Phys. Rev. **96**, 191 (1954).

[2] S. L. Glashow, "Partial Symmetries Of Weak Interactions," Nucl. Phys. **22**, 579 (1961).

[3] S. Weinberg, "A Model Of Leptons," Phys. Rev. Lett. **19**, 1264 (1967).

[4] A. Salam, "Weak and Electromagnetic Interactions," Conf. Proc. **C680519**, 367-377 (1968).

[5] E. D. Bloom *et al.*, "High-Energy Inelastic E P Scattering At 6-Degrees And 10-Degrees," Phys. Rev. Lett. **23**, 930 (1969).

[6] M. Breidenbach *et al.*, "Observed Behavior Of Highly Inelastic Electron-Proton Scattering," Phys. Rev. Lett. **23**, 935 (1969).

[7] R. Brandelik *et al.* [TASSO Collaboration], "Evidence for Planar Events in e+ e- Annihilation at High-Energies," Phys. Lett. B **86**, 243 (1979).

[8] M. E. Peskin and D. V. Schroeder, *An introduction to quantum field theory*, (Westview Press, 1995), Secion 17.6.

[9] J. J. Aubert *et al.* [E598 Collaboration], "Experimental Observation Of A Heavy Particle J," Phys. Rev. Lett. **33**, 1404 (1974).

[10] J. E. Augustin *et al.* [SLAC-SP-017 Collaboration], "Discovery Of A Narrow Resonance In E+ E- Annihilation," Phys. Rev. Lett. **33**, 1406 (1974).

[11] S. W. Herb *et al.*, "Observation of a dimuon resonance at 9.5-GeV in 400-GeV proton - nucleus Phys. Rev. Lett. **39**, 252 (1977).

[12] F. Abe *et al.* [CDF Collaboration], "Observation of top quark production in $\bar{p}p$ collisions," Phys. Rev. Lett. **74**, 2626 (1995) [hep-ex/9503002].

[13] S. Abachi *et al.* [D0 Collaboration], "Search for high mass top quark production in $p\bar{p}$ collisions at $\sqrt{s} = 1.8$ TeV," Phys. Rev. Lett. **74**, 2422 (1995) [hep-ex/9411001].

[14] D. J. Gross and F. Wilczek, "Ultraviolet Behavior of Nonabelian Gauge Theories," Phys. Rev. Lett. **30**, 1343 (1973).

[15] H. D. Politzer, "Reliable Perturbative Results for Strong Interactions?," Phys. Rev. Lett. **30**, 1346 (1973).

[16] S. G. Gorishnii, A. L. Kataev and S. A. Larin, "The O (alpha-s**3) corrections to sigma-tot (e+ e- $\rightarrow$ hadrons) and Gamma Phys. Lett. B **259**, 144 (1991).

[17] S. B. Rüster, V. Werth, M. Buballa, I. A. Shovkovy and D. H. Rischke, "The Phase diagram of neutral quark matter: Self-consistent treatment of quark masses," Phys. Rev. D **72**, 034004 (2005) [hep-ph/0503184].

[18] K. Rajagopal and F. Wilczek, "The Condensed matter physics of QCD," In *Shifman, M. (ed.): At the frontier of particle physics, vol. 3* 2061-2151, (World Scientific, 2000) [hep-ph/0011333].

[19] B. Muller, "Quark matter 2005: Theoretical summary," nucl-th/0508062.

[20] M. Gyulassy and L. McLerran, "New forms of QCD matter discovered at RHIC," Nucl. Phys. A **750**, 30 (2005) [nucl-th/0405013].

[21] G. Aad *et al.* [Atlas Collaboration], "Observation of a Centrality-Dependent Dijet Asymmetry in Lead-Lead Collisions at sqrt(S(NN))= 2.76 TeV with the ATLAS Detector at the LHC," Phys. Rev. Lett. **105**, 252303 (2010) [arXiv:1011.6182 [hep-ex]].

[22] J. D. Walecka, *Theoretical nuclear and subnuclear physics* (2 ed.), (World Scientific, 2004), p. 18.

[23] D. Durand, E. Suraud, B. Tamain, *Nuclear dynamics in the nucleonic regime*, (CRC Press, 2001), p. 4.

[24] B. Kiziltan, A. Kottas and S. E. Thorsett, "The Neutron Star Mass Distribution," arXiv:1011.4291 [astro-ph.GA].

[25] P. Haensel, A. Y. Potekhin, D. G. Yakovlev, *Neutron Stars 1: Equation of State and Structure*, (Springer, 2007).

[26] N. Chamel and P. Haensel, "Physics of Neutron Star Crusts," Living Rev. Rel. **11**, 10 (2008) [arXiv:0812.3955 [astro-ph]].

[27] J. M. Lattimer and M. Prakash, "Neutron Star Structure and the Equation of State," Astrophys. J. **550**, 426 (2001) [arXiv:astro-ph/0002232].

[28] J. M. Lattimer and M. Prakash, "Neutron Star Observations: Prognosis for Equation of State Constraints," Phys. Rept. **442**, 109 (2007) [astro-ph/0612440].

[29] F. Weber, *Pulsars as Astrophysical Laboratories for Nuclear and Particle Physics* (IOP Publishing Ltd., Bristol, 1999).

[30] B. C. Barrois, "Superconducting Quark Matter," Nucl. Phys. B **129**, 390 (1977).

[31] S. C. Frautschi, "Asymptotic Freedom And Color Superconductivity In Dense Quark Matter," CALT-68-701.

[32] B. C. Barrois, "Nonperturbative Effects In Dense Quark Matter," UMI-79-04847, (1979).

[33] D. Bailin and A. Love, "Superfluidity In Ultrarelativistic Quark Matter," Nucl. Phys. B **190**, 175 (1981).

[34] D. Bailin and A. Love, "Superconductivity In Quark Matter," Nucl. Phys. B **205**, 119 (1982).

[35] D. Ivanenko and D. F. Kurdgelaidze, "Remarks on quark stars," Lett. Nuovo Cim. IIS **1**, 13 (1969)

[36] D. D. Ivanenko and D. F. Kurdgelaidze, "Quark stars," Sov. Phys. J. **13**, 1015 (1970) [Izv. Vuz. Fiz. **13**, 39 (1970)].

[37] D. Bailin and A. Love, "Superfluid Quark Matter," J. Phys. A **12**, L283 (1979).

[38] M. Iwasaki, "Pairing correlation in quark matter," Prog. Theor. Phys. Suppl. **120**, 187 (1995).

[39] M. Iwasaki and T. Iwado, "Superconductivity in the quark matter," Phys. Lett. B **350**, 163 (1995).

[40] M. G. Alford, K. Rajagopal and F. Wilczek, "QCD at finite baryon density: Nucleon droplets and color superconductivity," Phys. Lett. B **422**, 247 (1998) [hep-ph/9711395].

[41] R. Rapp, T. Schäfer, E. V. Shuryak and M. Velkovsky, "Diquark Bose condensates in high density matter and instantons," Phys. Rev. Lett. **81**, 53 (1998) [hep-ph/9711396].

[42] D. Bailin and A. Love, "Superfluidity and Superconductivity in Relativistic Fermion Systems," Phys. Rept. **107**, 325 (1984).

[43] S. D. H. Hsu, "Color superconductivity in high density quark matter," hep-ph/0003140.

[44] M. G. Alford, "Color superconducting quark matter," Ann. Rev. Nucl. Part. Sci. **51**, 131 (2001) [hep-ph/0102047].

[45] D. K. Hong, "Aspects of color superconductivity," Acta Phys. Polon. B **32**, 1253 (2001) [hep-ph/0101025].

[46] G. Nardulli, "Effective description of QCD at very high densities," Riv. Nuovo Cim. **25N3**, 1 (2002) [hep-ph/0202037].

[47] S. Reddy, "Novel phases at high density and their roles in the structure and evolution of neutron stars," Acta Phys. Polon. B **33**, 4101 (2002) [nucl-th/0211045].

[48] T. Schäfer, "Quark matter," hep-ph/0304281.

[49] H. -c. Ren, "Color superconductivity of QCD at high baryon density," hep-ph/0404074.

[50] D. H. Rischke, "The Quark gluon plasma in equilibrium," Prog. Part. Nucl. Phys. **52**, 197 (2004) [nucl-th/0305030].

[51] M. Buballa, "NJL model analysis of quark matter at large density," Phys. Rept. **407**, 205 (2005) [hep-ph/0402234].

[52] M. Huang, "Color superconductivity at moderate baryon density," Int. J. Mod. Phys. E **14**, 675 (2005) [hep-ph/0409167].

[53] I. A. Shovkovy, "Two lectures on color superconductivity," Found. Phys. **35**, 1309 (2005) [nucl-th/0410091].

[54] M. G. Alford, A. Schmitt, K. Rajagopal and T. Schäfer, "Color superconductivity in dense quark matter," Rev. Mod. Phys. **80**, 1455 (2008) [arXiv:0709.4635 [hep-ph]].

[55] M. G. Alford, K. Rajagopal and F. Wilczek, "Color flavor locking and chiral symmetry breaking in high density QCD," Nucl. Phys. B **537**, 443 (1999) [hep-ph/9804403].

[56] D. T. Son, "Superconductivity by long range color magnetic interaction in high density quark matter," Phys. Rev. D **59**, 094019 (1999) [hep-ph/9812287].

[57] D. K. Hong, V. A. Miransky, I. A. Shovkovy and L. C. R. Wijewardhana, "Schwinger-Dyson approach to color superconductivity in dense QCD," Phys. Rev. D **61**, 056001 (2000) [Erratum-ibid. D **62**, 059903 (2000)] [hep-ph/9906478].

[58] T. Schäfer and F. Wilczek, "Superconductivity from perturbative one gluon exchange in high density quark matter," Phys. Rev. D **60**, 114033 (1999) [hep-ph/9906512].

[59] S. D. H. Hsu and M. Schwetz, "Magnetic interactions, the renormalization group and color superconductivity in high density QCD," Nucl. Phys. B **572**, 211 (2000) [hep-ph/9908310].

[60] R. D. Pisarski and D. H. Rischke, "Gaps and critical temperature for color superconductivity," Phys. Rev. D **61**, 051501 (2000) [nucl-th/9907041].

[61] R. D. Pisarski and D. H. Rischke, "Color superconductivity in weak coupling," Phys. Rev. D **61**, 074017 (2000) [nucl-th/9910056].

[62] I. A. Shovkovy and L. C. R. Wijewardhana, "On gap equations and color flavor locking in cold dense QCD with three massless flavors," Phys. Lett. B **470**, 189 (1999) [hep-ph/9910225].

[63] T. Schäfer, "Patterns of symmetry breaking in QCD at high baryon density," Nucl. Phys. B **575**, 269 (2000) [hep-ph/9909574].

[64] T. Schäfer, "Hard loops, soft loops, and high density effective field theory," Nucl. Phys. A **728**, 251 (2003) [hep-ph/0307074].

[65] R. D. Pisarski and D. H. Rischke, "A First order transition to, and then parity violation in, a color superconductor," Phys. Rev. Lett. **83**, 37 (1999) [nucl-th/9811104].

[66] C. Schmidt, "Lattice QCD at finite density," PoS LAT **2006**, 021 (2006) [hep-lat/0610116].

[67] Y. Nambu and G. Jona-Lasinio, "Dynamical Model of Elementary Particles Based on an Analogy with Superconductivity. 1.," Phys. Rev. **122**, 345 (1961).

[68] Y. Nambu and G. Jona-Lasinio, "Dynamical Model Of Elementary Particles Based On An Analogy With Superconductivity. Ii," Phys. Rev. **124**, 246 (1961).

[69] J. Bardeen, L. N. Cooper and J. R. Schrieffer, "Microscopic theory of superconductivity," Phys. Rev. **106**, 162 (1957).

[70] K. Rajagopal and A. Schmitt, "Stressed pairing in conventional color superconductors is unavoidable," Phys. Rev. D **73**, 045003 (2006) [hep-ph/0512043].

[71] M. G. Alford, J. Berges and K. Rajagopal, "Unlocking color and flavor in superconducting strange quark matter," Nucl. Phys. B **558**, 219 (1999) [hep-ph/9903502].

[72] R. D. Pisarski and D. H. Rischke, "Why color flavor locking is just like chiral symmetry breaking," nucl-th/9907094.

[73] M. Alford and S. Reddy, "Compact stars with color superconducting quark matter," Phys. Rev. D **67**, 074024 (2003) [nucl-th/0211046].

[74] T. Schäfer, "Quark hadron continuity in QCD with one flavor," Phys. Rev. D **62**, 094007 (2000) [hep-ph/0006034].

[75] A. Schmitt, Q. Wang and D. H. Rischke, "When the transition temperature in color superconductors is not like in BCS theory," Phys. Rev. D **66**, 114010 (2002) [nucl-th/0209050].

[76] M. Buballa, J. Hosek and M. Oertel, "Anisotropic admixture in color superconducting quark matter," Phys. Rev. Lett. **90**, 182002 (2003) [hep-ph/0204275].

[77] R. Rapp, T. Schäfer, E. V. Shuryak and M. Velkovsky, "High density QCD and instantons," Annals Phys. **280**, 35 (2000) [hep-ph/9904353].

[78] J. Madsen, "Probing strange stars and color superconductivity by r mode instabilities in millisecond pulsars," Phys. Rev. Lett. **85**, 10 (2000) [astro-ph/9912418].

[79] I. A. Shovkovy and P. J. Ellis, "Thermal conductivity of dense quark matter and cooling of stars," Phys. Rev. C **66**, 015802 (2002) [hep-ph/0204132].

[80] P. Jaikumar and M. Prakash, "Neutrino pair emission from Cooper pair breaking and recombination in superfluid quark matter," Phys. Lett. B **516**, 345 (2001) [astro-ph/0105225].

[81] P. Jaikumar, C. D. Roberts and A. Sedrakian, "Direct Urca neutrino rate in colour superconducting quark matter," Phys. Rev. C **73**, 042801 (2006) [nucl-th/0509093].

[82] A. Schmitt, I. A. Shovkovy and Q. Wang, "Neutrino emission and cooling rates of spin-one color superconductors," Phys. Rev. D **73**, 034012 (2006) [hep-ph/0510347].

[83] Q. Wang, Z. -g. Wang and J. Wu, "Phase space and quark mass effects in neutrino emissions in a color superconductor," Phys. Rev. D **74**, 014021 (2006) [hep-ph/0605092].

[84] M. G. Alford, J. Berges and K. Rajagopal, "Magnetic fields within color superconducting neutron star cores," Nucl. Phys. B **571**, 269 (2000) [hep-ph/9910254].

[85] E. V. Gorbar, "On color superconductivity in external magnetic field," Phys. Rev. D **62**, 014007 (2000) [hep-ph/0001211].

[86] I. A. Shovkovy and P. J. Ellis, "Optically opaque color flavor locked phase inside compact stars," Phys. Rev. C **67**, 048801 (2003) [hep-ph/0211049].

[87] C. Vogt, R. Rapp and R. Ouyed, "Photon emission from dense quark matter," Nucl. Phys. A **735**, 543 (2004) [hep-ph/0311342].

[88] D. T. Son, "Low-energy quantum effective action for relativistic superfluids," hep-ph/0204199.

[89] M. M. Forbes and A. R. Zhitnitsky, "Global strings in high density QCD," Phys. Rev. D **65**, 085009 (2002) [hep-ph/0109173].

[90] K. Iida and G. Baym, "Superfluid phases of quark matter. 3. Supercurrents and vortices," Phys. Rev. D **66**, 014015 (2002) [hep-ph/0204124].

[91] A. P. Balachandran, S. Digal and T. Matsuura, "Semi-superfluid strings in high density QCD," Phys. Rev. D **73**, 074009 (2006) [hep-ph/0509276].

[92] E. Nakano, M. Nitta and T. Matsuura, "Non-Abelian strings in high density QCD: Zero modes and interactions," Phys. Rev. D **78**, 045002 (2008) [arXiv:0708.4096 [hep-ph]].

[93] I. Shovkovy and M. Huang, "Gapless two flavor color superconductor," Phys. Lett. B **564**, 205 (2003) [hep-ph/0302142].

[94] M. Huang and I. Shovkovy, "Gapless color superconductivity at zero and at finite temperature," Nucl. Phys. A **729**, 835 (2003) [hep-ph/0307273].

[95] M. Alford, C. Kouvaris and K. Rajagopal, "Gapless color flavor locked quark matter," Phys. Rev. Lett. **92**, 222001 (2004) [hep-ph/0311286].

[96] M. Alford, M. Braby, M. W. Paris and S. Reddy, "Hybrid stars that masquerade as neutron stars," Astrophys. J. **629**, 969 (2005) [nucl-th/0411016].

[97] V. A. Miransky, I. A. Shovkovy and L. C. R. Wijewardhana, "The Effective potential of composite diquark fields and the spectrum of resonances in dense QCD," Phys. Lett. B **468**, 270 (1999) [hep-ph/9908212].

[98] C. Manuel, A. Dobado and F. J. Llanes-Estrada, "Shear viscosity in a CFL quark star," JHEP **0509**, 076 (2005) [hep-ph/0406058].

[99] G. Lugones and J. E. Horvath, "Color flavor locked strange matter," Phys. Rev. D **66**, 074017 (2002) [hep-ph/0211070].

[100] R. C. Tolman, "Static solutions of Einstein's field equations for spheres of fluid," Phys. Rev. **55**, 364 (1939).

[101] J. R. Oppenheimer and G. M. Volkoff, "On Massive neutron cores," Phys. Rev. **55**, 374 (1939).

[102] P. Demorest, T. Pennucci, S. Ransom, M. Roberts and J. Hessels, "Shapiro Delay Measurement of A Two Solar Mass Neutron Star," Nature **467**, 1081 (2010) [arXiv:1010.5788 [astro-ph.HE]].

[103] F. Özel, D. Psaltis, S. Ransom, P. Demorest and M. Alford, "The Massive Pulsar PSR J1614-2230: Linking Quantum Chromodynamics, Gamma-ray Bursts, and Gravitational Wave Astronomy," Astrophys. J. Lett. **724**, L199 (2010).

[104] P. Jaikumar, M. Prakash and T. Schäfer, "Neutrino emission from Goldstone modes in dense quark matter," Phys. Rev. D **66**, 063003 (2002) [astro-ph/0203088].

[105] S. Reddy, M. Sadzikowski and M. Tachibana, "Neutrino rates in color flavor locked quark matter," Nucl. Phys. A **714**, 337 (2003) [nucl-th/0203011].

[106] P. W. Anderson and N. Itoh, "Pulsar glitches and restlessness as a hard superfluidity phenomenon," Nature **256**, 25 (1975).

[107] I. Fushiki, E. H. Gudmundsson, and C. J. Pethick, “Surface structure of neutron stars with high magnetic fields," Astrophys. J. **342**, 958 (1989).

[108] G. Chanmugam, “Magnetic fields of degenerate stars,” Ann. Rev. Astron. Astrophys. **30**, 143 (1992).

[109] D. Lai, “Matter in strong magnetic fields,” Rev. Mod. Phys. **73**, 629 (2001) [astro-ph/0009333].

[110] C. Thompson and R. C. Duncan, “The Soft gamma repeaters as very strongly magnetized neutron stars. 2. Quiescent neutrino, x-ray, and Alfven wave emission,” Astrophys. J. **473**, 322 (1996).

[111] C. Y. Cardall, M. Prakash, and J. M. Lattimer, “Effects of strong magnetic fields on neutron star structure,” Astrophys. J. **554**, 322 (2001).

[112] E. J. Ferrer, V. de la Incera and C. Manuel, “Magnetic color flavor locking phase in high density QCD,” Phys. Rev. Lett. **95**, 152002 (2005) [hep-ph/0503162].

[113] E. J. Ferrer, V. de la Incera and C. Manuel, “Color-superconducting gap in the presence of a magnetic field,” Nucl. Phys. B **747**, 88 (2006) [hep-ph/0603233].

[114] E. J. Ferrer and V. de la Incera, “Magnetic Phases in Three-Flavor Color Superconductivity,” Phys. Rev. D **76**, 045011 (2007) [nucl-th/0703034 [NUCL-TH]].

[115] J. L. Noronha and I. A. Shovkovy, “Color-flavor locked superconductor in a magnetic field,” Phys. Rev. D **76**, 105030 (2007) [arXiv:0708.0307 [hep-ph]].

[116] K. Fukushima and H. J. Warringa, “Color superconducting matter in a magnetic field,” Phys. Rev. Lett. **100**, 032007 (2008) [arXiv:0707.3785 [hep-ph]].

[117] S. Fayazbakhsh and N. Sadooghi, “Color neutral 2SC phase of cold and dense quark matter in the presence of constant magnetic fields,” Phys. Rev. D **82**, 045010 (2010) [arXiv:1005.5022 [hep-ph]].

[118] S. Fayazbakhsh and N. Sadooghi, “Phase diagram of hot magnetized two-flavor color superconducting quark matter,” Phys. Rev. D **83**, 025026 (2011) [arXiv:1009.6125 [hep-ph]].

[119] E. J. Ferrer and V. de la Incera, “Magnetic fields boosted by gluon vortices in color superconductivity,” Phys. Rev. Lett. **97**, 122301 (2006) [hep-ph/0604136].

[120] E. J. Ferrer and V. de la Incera, “Chromomagnetic Instability and Induced Magnetic Field in Neutral Two-Flavor Color Superconductivity,” Phys. Rev. D **76**, 114012 (2007) [arXiv:0705.2403 [hep-ph]].

[121] B. Feng, D. Hou, H. -c. Ren and P. -p. Wu, "The Single Flavor Color Superconductivity in a Magnetic Field," Phys. Rev. Lett. **105**, 042001 (2010) [arXiv:0911.4997 [hep-ph]].

[122] L. Yu and I. A. Shovkovy, "Directional dependence of color superconducting gap in two-flavor QCD in a magnetic field," Phys. Rev. D (2012), in press [arXiv:1202.0872 [hep-ph]].

[123] M. Buballa and I. A. Shovkovy, "A Note on color neutrality in NJL-type models," Phys. Rev. D **72**, 097501 (2005).

[124] K. Iida, T. Matsuura, M. Tachibana and T. Hatsuda, "Melting pattern of diquark condensates in quark matter," Phys. Rev. Lett. **93**, 132001 (2004) [hep-ph/0312363].

[125] M. Alford, C. Kouvaris and K. Rajagopal, "Evaluating the gapless color-flavor locked phase," Phys. Rev. D **71**, 054009 (2005) [hep-ph/0406137].

[126] K. Fukushima, C. Kouvaris and K. Rajagopal, "Heating (gapless) color-flavor locked quark matter," Phys. Rev. D **71**, 034002 (2005) [hep-ph/0408322].

[127] M. Huang and I. A. Shovkovy, "Chromomagnetic instability in dense quark matter," Phys. Rev. D **70**, 051501 (2004) [hep-ph/0407049].

[128] M. Huang and I. A. Shovkovy, "Screening masses in neutral two-flavor color superconductor," Phys. Rev. D **70**, 094030 (2004) [hep-ph/0408268].

[129] R. Casalbuoni, R. Gatto, M. Mannarelli, G. Nardulli and M. Ruggieri, "Meissner masses in the gCFL phase of QCD," Phys. Lett. B **605**, 362 (2005) [Erratum-ibid. B **615**, 297 (2005)] [hep-ph/0410401].

[130] I. Giannakis and H. -C. Ren, "Chromomagnetic instability and the LOFF state in a two flavor color superconductor," Phys. Lett. B **611**, 137 (2005) [hep-ph/0412015].

[131] M. Alford and Q. -h. Wang, "Photons in gapless color-flavor-locked quark matter," J. Phys. G **31**, 719 (2005) [hep-ph/0501078].

[132] J. S. Schwinger, "On gauge invariance and vacuum polarization," Phys. Rev. **82**, 664 (1951).

[133] V. A. Miransky and I. A. Shovkovy, "Magnetic catalysis and anisotropic confinement in QCD," Phys. Rev. D **66**, 045006 (2002).

[134] U. W. Heinz, "Quark-gluon transport theory II. Color response and color correlations in a quark-gluon plasma," Annals Phys. **168**, 148 (1986).

[135] H. Vija and M. H. Thoma, "Braaten-Pisarski method at finite chemical potential," Phys. Lett. B **342**, 212 (1995).

[136] C. Manuel, "Hard dense loops in a cold nonAbelian plasma," Phys. Rev. D **53**, 5866 (1996).

[137] R. D. Pisarski, "Renormalized Gauge Propagator In Hot Gauge Theories," Physica A **158**, 146 (1989).

[138] M. Le Bellac, *Thermal Field Theory* (Cambridge University Press, Cambridge, England, 1996).

[139] D. K. Hong, "Aspects of high density effective theory in QCD," Nucl. Phys. B **582**, 451 (2000) [hep-ph/9905523].

[140] D. K. Hong, "An Effective field theory of QCD at high density," Phys. Lett. B **473**, 118 (2000) [hep-ph/9812510].

[141] W. E. Brown, J. T. Liu and H. -c. Ren, "On the perturbative nature of color superconductivity," Phys. Rev. D **61**, 114012 (2000) [hep-ph/9908248].

[142] Q. Wang and D. H. Rischke, "How the quark selfenergy affects the color superconducting gap," Phys. Rev. D **65**, 054005 (2002) [nucl-th/0110016].

[143] E. V. Gorbar, V. A. Miransky and I. A. Shovkovy, "Normal ground state of dense relativistic matter in a magnetic field," Phys. Rev. D **83**, 085003 (2011) [arXiv:1101.4954 [hep-ph]].

[144] I. S. Gradshtein and I. M. Ryzhik, *Tables of Integrals, Series, and Products* (Academic Press, Orlando, 1980).

APPENDIX A

GAP EQUATION FOR VANISHING MAGNETIC FIELD

In this appendix, we present the derivation of the gap equation and present its solution in the 2SC phase in the absence of a magnetic field. To simplify the study of color-superconducting phases, it is more convenient to introduce Nambu-Gorkov spinors:

$$\bar{\Psi} = (\bar{\psi}, \bar{\psi}^C), \qquad \Psi = \begin{pmatrix} \psi \\ \psi^C \end{pmatrix}, \tag{A.1}$$

where ψ is the Dirac spinor for the quark field, and $\psi^C = C\bar{\psi}^T$ is the charge-conjugate spinor. $C = i\gamma^2\gamma^0$ is the charge-conjugation matrix. In this basis, the inverse free-quark propagator S_0^{-1} reads

$$S_0^{-1} = \begin{pmatrix} [G_0^+]^{-1} & 0 \\ 0 & [G_0^-]^{-1} \end{pmatrix}, \tag{A.2}$$

where the inverse Dirac propagators for quarks ($[G_0^+]^{-1}$) and charge-conjugate quarks ($[G_0^-]^{-1}$) are given by

$$[G_0^\pm]^{-1} = i\gamma^\mu\partial_\mu \pm \mu\gamma^0 - m. \tag{A.3}$$

When the Cooper pairing is considered for quark quasiparticles in the color-superconducting phases, the full inverse quark propagator S^{-1} in the Nambu-Gorkov basis also has nonzero off-diagonal components and it reads

$$S^{-1} = \begin{pmatrix} [G_0^+]^{-1} & \Delta^- \\ \Delta^+ & [G_0^-]^{-1} \end{pmatrix}, \tag{A.4}$$

where $\Delta^- = -i\epsilon^{ab3}\epsilon_{ij3}\gamma^5\Delta$ and $\Delta^+ = \gamma^0(\Delta^-)^\dagger\gamma^0 = -i\epsilon^{ab3}\epsilon_{ij3}\gamma^5\Delta^*$ are the gap matrices in the 2SC phase, determined by the color-flavor-Dirac structure in Eq. (1.9). Note also that Δ^- and Δ^+ are off-diagonal elements of the quark self-energy. For simplicity, we neglect the diagonal parts of the quark self-energy, since they are not so important in the gap equation. They just give rise to an overall wave function renormalization factor (for details, see Refs. [141, 142]).

Starting from the inverse propagator in Eq. (A.4), one can invert it to obtain the full quark propagator

$$S = \begin{pmatrix} G^+ & \Xi^- \\ \Xi^+ & G^- \end{pmatrix}, \tag{A.5}$$

where

$$G^\pm = [(G_0^\pm)^{-1} - \Delta^\mp G_0^\mp \Delta^\pm]^{-1}, \tag{A.6}$$

$$\Xi^\pm = -G_0^\mp \Delta^\pm G^\pm. \tag{A.7}$$

The 21-component Ξ^+ (12-component Ξ^-) of the full quark propagator can be thought of as describing the propagation of a charge-conjugate quark (a quark) with propagator G_0^- (G_0^+) that is converted to a particle (a charge-conjugate quark) with propagator G^+ (G^-), via the condensate Δ^+ (Δ^-). Either of the off-diagonal components can be used to calculate the value of the gap parameter.

In the case of quark matter at asymptotic densities, the standard method for studying the gap parameter is the method of the Schwinger-Dyson equation. It is given by

$$S^{-1} = S_0^{-1} + \Sigma, \tag{A.8}$$

where Σ is the self energy of the quark, defined in terms of the full quark and gluon propagators. In general, the complete calculation of the self energy Σ contains an infinite number of coupled equations for Green's functions and thus it is unsolvable exactly. However, since the dominant one-gluon interaction is weak at asymptotic densities, the leading-order contribution can be well described by the so-called improved rainbow approximation (one-loop approximation). In this approximation of the Schwinger-Dyson equation, one uses the bare quark-gluon vertices. Why do we call the rainbow approximation "improved"? This is because it goes beyond the simple rainbow approximation, in which the free gluon propagator is used and the

screening effects of the dense medium is usually neglected. Here, since the gluon interaction is partially screened by surrounding dense quark matter, the modification of the gluon propagator should be taken into consideration. It can be described in terms of the gluon self-energy Π, which is defined by the following relation:

$$D^{-1} = D_0^{-1} + \Pi, \tag{A.9}$$

where D^{-1} and D_0^{-1} are the full and free inverse gluon propagators, respectively, and Π is the gluon self-energy, or the polarization tensor. The Lorentz and color indices are suppressed in Eq. (A.9).

The main contribution to the polarization tensor comes from the quark loop with hard internal momenta near Fermi surface (of order μ). In other words, the gluons with soft momenta, less than $g\mu$, are most important in the formation of the diquark condensates. Compared to the other contributions, i.e., the ghost and the gluon loops, the contribution of the quark loops is large because it is proportional to the density of quark states around the Fermi surface (as well as to the coupling constant g^2), i.e., $\Pi \sim g^2\mu^2$. This approximation is called the hard dense loop (HDL) approximation [134, 135, 136] for the gluon propagator in the dense medium and it is further discussed in Sec. 2.4. The corresponding modified gluon propagator is given by Eq. (2.34) and it is used for the calculation of the gap parameter here.

In the improved rainbow approximation, the Schwinger-Dyson equation for quark propagator in momentum space reads

$$S^{-1}(K) = S_0^{-1}(K) + ig^2 \int \frac{d^4p}{(2\pi)^4} \Gamma_\mu^A S(P) \Gamma_\nu^B D_{AB}^{\mu\nu}(K-P), \tag{A.10}$$

where the bare quark-gluon vertices in the Nambu-Gorkov basis are given by

$$\Gamma_\mu^A = \gamma_\mu \begin{pmatrix} T^A & 0 \\ 0 & -(T^A)^T \end{pmatrix}. \tag{A.11}$$

By using the expressions in Eqs. (A.2) and (A.4), we see that the 21-component of $\Sigma(K)$ is the gap matrix $\Delta^+(K)$. Now, we concentrate on the study of 21-components of Eq. (A.10). It reduces to the well known gap equation in the 2SC phase [56, 57, 58, 59, 60, 61],

$$\Delta^+(K) = ig^2 \int \frac{d^4p}{(2\pi)^4} \gamma_\mu (-T^A)^T \Xi^+ \gamma_\nu T^B D^{\mu\nu}_{AB}(K-P). \tag{A.12}$$

After performing the explicit calculation on the matrix Ξ^+ and momentum integration, we obtain the following approximate form of the gap equation in Euclidean space (the dependence of the gap on the three-momentum is conventionally neglected) [56, 57, 58, 59, 60, 61, 62, 63, 64, 139, 140],

$$\Delta(k_4) \simeq \frac{g^2}{36\pi^2} \int_{-\infty}^{\infty} dp_4 \frac{\Delta(p_4)}{\sqrt{(p_4)^2 + (\Delta)^2}} \ln \frac{\Lambda}{|k_4 - p_4|}, \tag{A.13}$$

where $k_4 = ik_0$, $p_4 = ip_0$, and $\Lambda = 4(2\mu)^3/(\pi m_D^2)$.

In order to solve the integral equation Eq. (A.13) rigorously, we can use the method in Ref. [57]. In the leading logarithm approximation, we can rewrite Eq. (A.13) as follows:

$$\Delta(y) \approx \bar{g}^2 \int_0^y \frac{dx\Delta(x)}{\sqrt{x^2 + |\Delta|^2}} \ln \frac{\Lambda}{y} + \bar{g}^2 \int_y^\Lambda \frac{dx\Delta(x)}{\sqrt{x^2 + |\Delta|^2}} \ln \frac{\Lambda}{x} \tag{A.14}$$

where, by definition, $y \equiv k_4$, $x \equiv p_4$, $|\Delta| \equiv \Delta(0)$, and $\bar{g}^2 = g^2/18\pi^2$. And Λ is used as an ultraviolet cutoff for the integration. We can easily find that this equation is equivalent to the differential equation,

$$y\Delta''(y) + \Delta(x) + \bar{g}^2 \frac{\Delta(y)}{\sqrt{y^2 + |\Delta|^2}} = 0, \tag{A.15}$$

with the following infrared and ultraviolet boundary conditions:

$$y\Delta'(y)|_{y=0} = 0\ (IR), \quad \Delta(\Lambda) = 0\ (UV). \tag{A.16}$$

Then we solve the differential equation in two regions $y \ll |\Delta|$ and $y \gg |\Delta|$.

In the infrared region $y \ll |\Delta|$, the solution is given by the following Bessel function,

$$\Delta(y) \;=\; |\Delta| J_0\left(2\bar{g}\sqrt{\frac{y}{|\Delta|}}\right). \tag{A.17}$$

And in the ultraviolet region, the solution reads

$$\Delta(y) \;=\; C\sin\left(\bar{g}\ln\frac{\Lambda}{y}\right). \tag{A.18}$$

Finally, matching the solutions and their derivatives ate the point $y = |\Delta|$, we arrive at the analytical expression for the gap parameter,

$$|\Delta| \;=\; \Lambda\exp\left[-\frac{1}{\bar{g}}\arctan\left(\frac{J_0(2\bar{g})}{J_1(2\bar{g})}\right)\right], \tag{A.19}$$

and determine the value of the constant C:

$$C = |\Delta|\sqrt{J_0^2(2\bar{g}) + J_1^2(2\bar{g})}. \tag{A.20}$$

If the couping constant is very small, $\bar{g} \ll 1$, we find that

$$|\Delta| \;\approx\; \Lambda\exp\left(1 - \frac{\pi}{2\bar{g}}\right) = \Lambda\exp\left(1 - \frac{\pi}{2\bar{g}}\right). \tag{A.21}$$

Thus, the approximate solution to Eq. (A.13) reads

$$\Delta^{(0)} \simeq \Lambda\exp(-\frac{3\pi^2}{\sqrt{2}g} + 1). \tag{A.22}$$

APPENDIX B

QUARK PROPAGATOR IN MAGNETIC FIELD

In this appendix we calculate the explicit forms of the full propagators for quasiparticles with $\tilde{Q} = +\frac{1}{2}$ charge. (The result can be also easily generalized to quasiparticles with $\tilde{Q} = -\frac{1}{2}$ charge.) We present the details of the analysis for 11- and 21-components of the propagator $S^X_{(+\frac{1}{2})}$.

The starting point of the derivation is the definition of the inverse propagator in Eq. (2.27). By making use of Eqs. (A.5) – (A.7), the explicit forms of the 11- and 21-components of the propagator $S^X_{(+\frac{1}{2})}$ read

$$\begin{aligned} S^X_{(+\frac{1}{2})11} &= \left(\gamma^\mu \pi_\mu^{(+\frac{1}{2})} - \mu_{dg}\gamma^0 + m\right)\Big[\left(\gamma^\mu \pi_\mu^{(+\frac{1}{2})} + \mu_{ur}\gamma^0 - m\right) \\ &\quad \times \left(\gamma^\mu \pi_\mu^{(+\frac{1}{2})} - \mu_{dg}\gamma^0 + m\right) - \Delta^2\Big]^{-1}, \qquad \text{(B.1)} \\ S^X_{(+\frac{1}{2})21} &= -i\gamma^5\Delta^*\left[\left(\gamma^\mu \pi_\mu^{(+\frac{1}{2})} + \mu_{ur}\gamma^0 - m\right)\left(\gamma^\mu \pi_\mu^{(+\frac{1}{2})} - \mu_{dg}\gamma^0 + m\right) - \Delta^2\right]^{-1}, \end{aligned}$$

(B.2)

where, by definition, $\pi_\mu^{(\tilde{Q})} \equiv i\partial_\mu + \tilde{e}\tilde{Q}\tilde{A}_\mu$ and the gauge field is $\tilde{A}^\mu = (0, 0, x\tilde{B}, 0)$ with the strength of the external (rotated) magnetic field denoted by $\tilde{B}$.

The inverse of the operator in the square brackets of Eqs. (B.1) and (B.2), which is the same for all components of the propagator, can be calculated by employing the usual trick of “quadrating" the operator. In this case, however, we end up “bi-quadrating" it because the corresponding operator is already quadratic in energy. For this purpose, let us introduce the following shorthand notation:

$$\begin{aligned} \hat{X}^\pm &= \left[(i\partial_t - \delta\mu)^2 - \boldsymbol{\pi}_\perp^2 - i\tilde{e}\tilde{Q}\tilde{B}\gamma^1\gamma^2 - (\pi^3)^2 - m^2 - \bar{\mu}^2 - \Delta^2\right] \\ &\quad \pm \; 2\gamma^0\bar{\mu}\left(\boldsymbol{\gamma}_\perp \cdot \boldsymbol{\pi}_\perp + \gamma^3\pi^3 - m\right), \qquad \text{(B.3)} \end{aligned}$$

where $\delta\mu = \frac{\mu_{dg}-\mu_{ur}}{2}$, $\bar{\mu} = \frac{\mu_{ur}+\mu_{dg}}{2}$, $\boldsymbol{\pi}_\perp = (\pi^1, \pi^2)$ and $\boldsymbol{\gamma}_\perp = (\gamma^1, \gamma^2)$. Note that $\hat{X}^-$ is the same operator that appears in the square brackets of Eqs. (B.1) and (B.2). For simplicity of notation, we dropped index $\tilde{Q}$ here.

Let us first concentrate on the 11-component of the propagator. It can be rewritten as follows:

$$\begin{aligned} S^X_{(+\frac{1}{2})11} &= \left(\gamma^\mu \pi_\mu^{(+\frac{1}{2})} - \mu_{dg}\gamma^0 + m\right) \hat{X}^+ \left(\hat{X}^- \hat{X}^+\right)^{-1} \\ &\equiv \left(\hat{A} - \boldsymbol{\gamma}_\perp \cdot \boldsymbol{\pi}_\perp \hat{B}\right) \hat{C}^{-1}. \end{aligned} \tag{B.4}$$

The three new operator functions introduced here are defined by

$$\begin{aligned} \hat{A} &= \Big[(i\partial_t)\gamma^0 - \pi^3\gamma^3 - \mu_{dg}\gamma^0 + m\Big]\Big[(i\partial_t - \delta\mu)^2 - \bar{\mu}^2 - 2\bar{\mu}(\gamma^3\pi^3 + m)\gamma^0 - (\pi^3)^2 \\ &\quad -m^2 - \Delta^2\Big] - \Big[(i\partial_t)\gamma^0 - \pi^3\gamma^3 + \mu_{ur}\gamma^0 + m\Big]\Big(\boldsymbol{\pi}_\perp^2 + i\tilde{e}\tilde{Q}\tilde{B}\gamma^1\gamma^2\Big), \end{aligned} \tag{B.5}$$

$$\hat{B} = (i\partial_t - \mu_{dg})^2 - \boldsymbol{\pi}_\perp^2 - i\tilde{e}\tilde{Q}\tilde{B}\gamma^1\gamma^2 - (\pi^3)^2 - m^2 - \Delta^2, \tag{B.6}$$

$$\begin{aligned} \hat{C} &= \Big[(i\partial_t - \delta\mu)^2 - \boldsymbol{\pi}_\perp^2 - i\tilde{e}\tilde{Q}\tilde{B}\gamma^1\gamma^2 - (\pi^3)^2 - m^2 + \bar{\mu}^2 - \Delta^2\Big]^2 \\ &\quad -4\bar{\mu}^2\Big[(i\partial_t - \delta\mu)^2 - \Delta^2\Big]. \end{aligned} \tag{B.7}$$

In the coordinate space, the corresponding propagator is formally given by

$$S^X_{(+\frac{1}{2})11}(u,u') = \left\langle u \middle| \left(\hat{A} - \boldsymbol{\gamma}_\perp \cdot \boldsymbol{\pi}_\perp \hat{B}\right) \hat{C}^{-1} \middle| u' \right\rangle, \tag{B.8}$$

where $u = (t, z, \boldsymbol{r}_\perp)$ and $\boldsymbol{r}_\perp = (x, y)$. It is easy to perform a Fourier transform in time and z-coordinate,

$$S^X_{(+\frac{1}{2})11}(\omega, k^3; \boldsymbol{r}_\perp, \boldsymbol{r}'_\perp) = \int dt\, dz\, e^{i\omega t - ik^3 z}\, S^1_{(+\frac{1}{2})11}(u,u'). \tag{B.9}$$

In essence, this transform results in a simple replacement of $i\partial_t \to \omega$ and $\pi^3 \to k^3$ in all of the earlier expressions.

To proceed further, we should find a basis of suitable eigenstates in which the propagator has the simplest possible form. To this end, we note that the functions $\hat{A}$, $\hat{B}$ and $\hat{C}$ depend on the operator $\boldsymbol{\pi}_\perp^2 + i\tilde{e}\tilde{Q}\tilde{B}\gamma^1\gamma^2$. Its eigenvalues are well known: $2n|\tilde{e}\tilde{Q}\tilde{B}|$, where $n = 0, 1, 2, \ldots$ is the Landau-level index. Note that the integer quantum number n has both orbital and spin contributions, i.e., $n = k + (1+s)/2$,

where $k = 0, 1, 2, \ldots$ labels a specific orbital state, while $s = \pm 1$ corresponds to a given (up or down) spin state. The explicit form of the corresponding eigenstates $\langle \boldsymbol{r}_\perp | k\, p_y\, s \rangle$ is also well known (e.g., see Ref. [143], where similar method and notations are used).

Following closely the approach of Ref. [143], we use the complete set of eigenstates to simplify the expression for the propagator (B.9). The final result will have the form

$$S^X_{(+\frac{1}{2})21}(\omega, k^3; \boldsymbol{r}_\perp, \boldsymbol{r}'_\perp) = e^{i\Phi(\boldsymbol{r}_\perp, \boldsymbol{r}'_\perp)} \bar{S}^X_{(+\frac{1}{2})21}(\omega, k^3; \boldsymbol{r}_\perp - \boldsymbol{r}'_\perp), \tag{B.10}$$

where $\Phi(\boldsymbol{r}_\perp, \boldsymbol{r}'_\perp)$ is the Schwinger phase. In the Landau gauge used, the explicit form of the phase is

$$\Phi(\boldsymbol{r}_\perp, \boldsymbol{r}'_\perp) = -\frac{(x + x')(y - y')}{2l^2} \mathrm{sign}(\tilde{e}\tilde{Q}\tilde{B}), \tag{B.11}$$

where $l = 1/\sqrt{|\tilde{e}\tilde{Q}\tilde{B}|}$ is the magnetic length. (Note that this phase is responsible for breaking the translational invariance of the propagator.) The translationally invariant part of the propagator is given by

$$\begin{aligned} \bar{S}^X_{(+\frac{1}{2})11}(\omega, k^3; \boldsymbol{r}_\perp) \;=\; & \frac{e^{-\xi/2}}{2\pi l^2} \sum_{n=0}^{\infty} \left\{ \frac{\mathcal{A}_n}{\mathcal{C}_n} \Big[L_n(\xi)\mathcal{P}_- + L_{n-1}(\xi)\mathcal{P}_+ \Big] - i \frac{\boldsymbol{\gamma}_\perp \cdot \boldsymbol{r}_\perp}{l^2} \right. \\ & \left. \times \frac{\mathcal{B}_n}{\mathcal{C}_n} L^1_{n-1}(\xi) \right\}, \end{aligned} \tag{B.12}$$

where $\xi \equiv \boldsymbol{r}^2_\perp/(2l^2)$, $L^\alpha_n(\xi)$ are the generalized Laguerre polynomials (by definition, $L_n \equiv L^0_n$ and $L^\alpha_{-1} = 0$), and

$$\mathcal{P}_\pm = \frac{1}{2} \Big(1 \pm i\gamma^1\gamma^2 \mathrm{sign}(\tilde{e}\tilde{Q}\tilde{B}) \Big) \tag{B.13}$$

are the spin projection operators.

Functions $\mathcal{A}_n$, $\mathcal{B}_n$ and $\mathcal{C}_n$ in Eq. (B.12) replace the corresponding operators $\hat{A}$, $\hat{B}$ and $\hat{C}$, when projected onto the nth Landau-level state. Their explicit forms

are obtained from $\hat{A}$, $\hat{B}$ and $\hat{C}$ by replacing $\boldsymbol{\pi}_\perp^2 + i\tilde{e}\tilde{Q}\tilde{B}\gamma^1\gamma^2 \to 2n|\tilde{e}\tilde{Q}\tilde{B}|$, i.e.,

$$\begin{aligned}
\mathcal{A}_n &= \Big[\omega\gamma^0 - k^3\gamma^3 - \mu_{dg}\gamma^0 + m\Big]\Big[\big(\omega - \delta\mu\big)^2 - \bar{\mu}^2 - 2\bar{\mu}(\gamma^3 k^3 + m)\gamma^0 \\
&\quad -(k^3)^2 - m^2 - \Delta_n^2\Big] - 2n|\tilde{e}\tilde{Q}\tilde{B}|\big[\omega\gamma^0 - k^3\gamma^3 + \mu_{ur}\gamma^0 + m\big], \qquad \text{(B.14)} \\
\mathcal{B}_n &= (\omega - \mu_{dg})^2 - 2n|\tilde{e}\tilde{Q}\tilde{B}| - (k^3)^2 - m^2 - \Delta_n^2, \qquad \text{(B.15)} \\
\mathcal{C}_n &= \Big[\big(\omega - \delta\mu\big)^2 - 2n|\tilde{e}\tilde{Q}\tilde{B}| - (k^3)^2 - m^2 + \bar{\mu}^2 - \Delta_n^2\Big]^2 \\
&\quad -4\bar{\mu}^2\Big[\big(\omega - \delta\mu\big)^2 - \Delta_n^2\Big]. \qquad \text{(B.16)}
\end{aligned}$$

Here we consider a general case when the dynamically generated gap function Δ_n depends not only on the energy ω and k^3, but also on the Landau-level index n. (In operator form, it means that Δ depends on $\boldsymbol{\pi}_\perp^2 + i\tilde{e}\tilde{Q}\tilde{B}\gamma^1\gamma^2$.) Therefore, we replaced the operator Δ with the corresponding value Δ_n that it takes in the nth Landau-level state.

At this point, it may be appropriate to note that the zeros of $\mathcal{C}_n$ determine the spectrum of quasiparticles in color-superconducting quark matter in a magnetic field, i.e.,

$$E_{n,\pm,\pm} = \delta\mu \pm \sqrt{\left[\sqrt{2n|\tilde{e}\tilde{Q}\tilde{B}| + (k^3)^2 + m^2} \pm \bar{\mu}\right]^2 + \Delta_n^2}. \qquad \text{(B.17)}$$

Note that all four different sign combinations are possible. The choice of the sign in front of the chemical potential $\bar{\mu}$ corresponds to the choice of either particle states (allowing small energies of order Δ_n) or antiparticle states (generally having large energies of order $\bar{\mu}$). The sign in front of the overall square root corresponds to particle/hole type quasiparticles (i.e., positive/negative energy states). One should note, however, that an additional complication in this classification appears in the case of gapless superconducting phases when $\delta\mu > \Delta_n$ [93, 94, 95, 125, 126].

Following the same approach, we can derive explicit expressions for all components of the propagator $S^X_{(+\frac{1}{2})}$. For example, the final expression for the off-

diagonal 21-component, which is used in the gap equation in the main text, reads

$$S^X_{(+\frac{1}{2})21}(\omega,k^3;\boldsymbol{r}_\perp,\boldsymbol{r}'_\perp)=e^{i\Phi(\boldsymbol{r}_\perp,\boldsymbol{r}'_\perp)}\bar{S}^X_{(+\frac{1}{2})21}(\omega,k^3;\boldsymbol{r}_\perp-\boldsymbol{r}'_\perp), \tag{B.18}$$

with the translationally invariant part given by

$$\begin{aligned}\bar{S}^X_{(+\frac{1}{2})21}(\omega,k^3;\boldsymbol{r}_\perp) &= -i\gamma^5\frac{e^{-\xi/2}}{2\pi l^2}\sum_{n=0}^{\infty}\Delta_n^*\Big\{\frac{\mathcal{E}_n}{\mathcal{C}_n}[L_n(\xi)\mathcal{P}_-+L_{n-1}(\xi)\mathcal{P}_+]\\ &\quad -i\frac{\boldsymbol{\gamma}_\perp\cdot\boldsymbol{r}_\perp}{l^2}\frac{2\bar{\mu}\gamma^0}{\mathcal{C}_n}L^1_{n-1}(\xi)\Big\}.\end{aligned} \tag{B.19}$$

Here we introduced yet another function,

$$\mathcal{E}_n=(\omega-\delta\mu)^2-2n|\tilde{e}\tilde{Q}\tilde{B}|-(k^3)^2-m^2-\bar{\mu}^2-\Delta_n^2-2\bar{\mu}(k^3\gamma^3+m)\gamma^0. \tag{B.20}$$

Before concluding this appendix, let us add that similar representations can be also derived for the components of the inverse propagator. As an example, let us present the corresponding result for $\left[S^X_{(+\frac{1}{2})}\right]^{-1}_{21}(u,u')$, which is used in the gap equation. It has the same general structure as the above expressions for the components of $S^X_{(+\frac{1}{2})}$, i.e.,

$$\left[S^X_{(+\frac{1}{2})}\right]^{-1}_{21}(\omega,k^3;\boldsymbol{r}_\perp,\boldsymbol{r}'_\perp)=e^{i\Phi(\boldsymbol{r}_\perp,\boldsymbol{r}'_\perp)}\left[\overline{S^X}_{(+\frac{1}{2})}\right]^{-1}_{21}(\omega,k^3;\boldsymbol{r}_\perp-\boldsymbol{r}'_\perp). \tag{B.21}$$

It is important that the inverse propagator has exactly the same phase as the propagator itself, see Eqs. (B.10) and (B.11). The explicit form of its translationally invariant part reads

$$\left[\overline{S^X}_{(+\frac{1}{2})}\right]^{-1}_{21}(\omega,k^3;\boldsymbol{r}_\perp)=-i\gamma^5\frac{e^{-\xi/2}}{2\pi l^2}\sum_{n=0}^{\infty}\Delta_n^*\left[L_n(\xi)\mathcal{P}_-+L_{n-1}(\xi)\mathcal{P}_+\right]. \tag{B.22}$$

APPENDIX C

GAP EQUATION IN MAGNETIC FIELD

The gap equation (i.e., the off-diagonal component of the Schwinger-Dyson equation for the full propagator) in the coordinate space reads

$$\left[S^X_{(\tilde{Q})}\right]^{-1}_{21}(u,u') = -ig^2\gamma^\mu \left(T^A\right)^T \left[S^X_{(\tilde{Q})}\right]_{21}(u,u')\gamma^\nu T^B D^{AB}_{\mu\nu}(u-u'), \qquad \text{(C.1)}$$

where $D^{AB}_{\mu\nu}(u,u')$ is the gluon propagator, which is assumed to be diagonal in adjoint color indices ($A,B = 1,2,...,8$), i.e., $D^{AB}_{\mu\nu}(u-u') = \delta^{AB}D_{\mu\nu}(u-u')$. By making use of the identity

$$\sum_{A=1}^{8} T^A_{a'a}T^A_{b'b} = \frac{1}{2}\delta_{a'b}\delta_{ab'} - \frac{1}{6}\delta_{aa'}\delta_{bb'}, \qquad \text{(C.2)}$$

we derive the following form of the gap equation:

$$\left[S^X_{(\tilde{Q})}\right]^{-1}_{21}(u,u') = i\frac{2}{3}g^2\gamma^\mu \left[S^X_{(\tilde{Q})}\right]_{21}(u,u')\gamma^\nu D_{\mu\nu}(u-u'). \qquad \text{(C.3)}$$

Taking into account that all components of the quasiparticle propagator as well as its inverse have the same nonzero Schwinger phase, we can derive the equation for the translationally invariant parts simply by dropping the common phase factor on both side of the gap equation,

$$\begin{aligned}\left[\overline{S^X}_{(+\frac{1}{2})}\right]^{-1}_{21}(\omega,k^3;\boldsymbol{r}_\perp) &= i\frac{2g^2}{3}\int\frac{d\omega' dk'^3}{(2\pi)^2}\gamma^\mu \bar{S}^X_{(+\frac{1}{2})21}(\omega,k^3;\boldsymbol{r}_\perp)\gamma^\nu \\ &\quad\times\int\frac{d^2\boldsymbol{q}_\perp}{(2\pi)^2}e^{i\boldsymbol{q}_\perp\cdot\boldsymbol{r}_\perp}D_{\mu\nu}(\omega-\omega',k^3-k'^3,\boldsymbol{q}_\perp), \qquad \text{(C.4)}\end{aligned}$$

where we additionally performed a Fourier transform in time and z-coordinate on both sides of the equation, and used a momentum representation for the gluon propagator.

By making use of the explicit form of the relevant translationally invariant parts of the propagators in Eqs. (B.19) and (B.22), we rewrite the last form of the

gap equation as follows:

$$\frac{e^{-\xi/2}}{2\pi l^2}\sum_{n=0}^{\infty}\Delta_n[L_n(\xi)\mathcal{P}_- + L_{n-1}(\xi)\mathcal{P}_+]$$
$$= -i\frac{2g^2}{3}\frac{e^{-\xi/2}}{2\pi l^2}\sum_{n=0}^{\infty}\int\frac{d\omega' dk'^3}{(2\pi)^2}\gamma^\mu\frac{\Delta_n}{\mathcal{C}_n}\Big\{\mathcal{E}_n\Big[L_n(\xi)\mathcal{P}_- + L_{n-1}(\xi)\mathcal{P}_+\Big] - 2\bar{\mu}i\frac{\boldsymbol{\gamma}_\perp\cdot\boldsymbol{r}_\perp}{l^2}$$
$$\times\gamma^0 L^1_{n-1}(\xi)\Big\}\gamma^\nu\int\frac{d^2\boldsymbol{q}_\perp}{(2\pi)^2}e^{i\boldsymbol{q}_\perp\cdot\boldsymbol{r}_\perp}D_{\mu\nu}(\omega-\omega', k^3-k'^3, \boldsymbol{q}_\perp). \quad \text{(C.5)}$$

The last equation can now be easily projected onto different orbital eigenstates. This is formally done by multiplying both sides of the equation by $e^{-\xi/2}L_m(\xi)$ (where $m = 0, 1, 2, \ldots$) and integrating over the perpendicular spatial coordinates $\boldsymbol{r}_\perp$. After performing such projections, we arrive at the following (infinite) set of gap equations in the Landau-level representation:

$$\Delta_m\mathcal{P}_- + \Delta_{m+1}\mathcal{P}_+ = -i\frac{2g^2}{3}\sum_{n=0}^{\infty}\int\frac{d\omega' dk'^3}{(2\pi)^2}\int\frac{d^2\boldsymbol{q}_\perp}{(2\pi)^2}\gamma^\mu\frac{\Delta_n\mathcal{E}_n}{\mathcal{C}_n}\Big[\mathcal{L}^{(0)}_{n,m}\left(\frac{q_\perp^2 l^2}{2}\right)\mathcal{P}_-$$
$$+\mathcal{L}^{(0)}_{n-1,m}\left(\frac{q_\perp^2 l^2}{2}\right)\mathcal{P}_+\Big]\gamma^\nu D_{\mu\nu}(\omega-\omega', k^3-k'^3, \boldsymbol{q}_\perp), \quad \text{(C.6)}$$

where, by definition,

$$\mathcal{L}^{(0)}_{n,m}(x) = (-1)^{n+m}e^{-x}L_n^{m-n}(x)\,L_m^{n-m}(x). \quad \text{(C.7)}$$

In the derivation, we used the following table integrals (see formulas 7.414 3 and 7.422 2 in Ref. [144]):

$$\int_0^\infty dx e^{-x}x^\alpha L^\alpha_m(x)L^\alpha_n(x) = \frac{\Gamma(n+\alpha+1)}{n!}\delta^n_m, \quad \text{(C.8)}$$

and

$$\int_0^\infty dx x^{2\sigma+1}e^{-\alpha x^2}L^\sigma_m(\alpha x^2)L^\sigma_n(\alpha x^2)J_0(xy)$$
$$= \frac{(-1)^{m+n}}{2\alpha^{\sigma+1}}\frac{(m+\sigma)!}{m!}e^{-y^2/4\alpha}L^{n-m}_{m+\sigma}\left(\frac{y^2}{4\alpha}\right)L^{m-n}_n\left(\frac{y^2}{4\alpha}\right). \quad \text{(C.9)}$$

APPENDIX D

PROPAGATOR IN WEAK MAGNETIC FIELD LIMIT

In this appendix, we consider the quasiparticle propagator in the limit of weak magnetic field.

We begin by performing a Fourier transform of the translation-invariant part of the propagator,

$$\begin{aligned}\bar{S}^X_{(+\frac{1}{2})21}(\omega,k^3,\boldsymbol{k}_\perp) &= \int d^2\boldsymbol{r}_\perp e^{-i\boldsymbol{k}_\perp\cdot\boldsymbol{r}_\perp}\bar{S}^X_{(+\frac{1}{2})21}(\omega,k^3;\boldsymbol{r}_\perp)\\ &= -2i\gamma^5 e^{-k_\perp^2 l^2}\sum_{n=0}^{\infty}(-1)^n\frac{\Delta_n}{\mathcal{C}_n}\Big\{\mathcal{E}_n\Big[L_n\big(2k_\perp^2l^2\big)\mathcal{P}_-\\ &\quad -L_{n-1}\big(2k_\perp^2l^2\big)\mathcal{P}_+\Big]+4\bar{\mu}(\boldsymbol{\gamma}_\perp\cdot\boldsymbol{k}_\perp)\gamma^0L^1_{n-1}\big(2k_\perp^2l^2\big)\Big\}\end{aligned} \tag{D.1}$$

In the weak field limit, the difference between the neighboring levels is vanishingly small in energy and the properties of the corresponding states become almost indistinguishable. In application to the gap function Δ_n, this means that it will become almost independent of the Landau-level index in a wide range of n near the (would-be) Fermi surface. (Strictly speaking, the true Fermi surface is not well defined in a superconductor, but if the gap is small, $\Delta \ll \bar{\mu}$, one could map the corresponding phase space onto the phase space in the free quark matter.)

In order to derive a weak-field expression for the propagator, one needs to first perform the sum over the Landau-level index n. A straightforward way of achieving this is to employ the usual proper-time representation, i.e.,

$$\frac{1}{(a+2n|b|)^2+c^2} = \int_0^\infty\frac{ds}{c}\sin(sc)e^{-s(a+2n|b|)}, \tag{D.2}$$

$$\frac{a+2n|b|}{(a+2n|b|)^2+c^2} = \int_0^\infty ds\cos(sc)e^{-s(a+2n|b|)}, \tag{D.3}$$

for the two types of structures appearing in the Euclidian propagator, and then use the well known summation formula for Laguerre polynomials,

$$\sum_{n=0}^{\infty}L_n^\alpha(x)z^n=(1-z)^{-(\alpha+1)}\exp\left(\frac{xz}{z-1}\right). \tag{D.4}$$

Before using these identities, it is convenient to rewrite propagator (D.1) in the following form:

$$\bar{S}^X_{(+\frac{1}{2})21}(i\omega_E, k^3, \boldsymbol{k}_\perp) = i\gamma^5\Delta\left[I_1 + 2\bar{\mu}(k^3\gamma^3 + m + \bar{\mu}\gamma^0)\gamma^0 I_2 + 2\bar{\mu}(\boldsymbol{\gamma}_\perp\cdot\boldsymbol{k}_\perp)\gamma^0 I_3\right], \tag{D.5}$$

where, by definition, the sums I_i ($i = 1, 2, 3$) are

$$\begin{aligned} I_1 &= 2e^{-\frac{k_\perp^2}{|b|}}\sum_{n=0}^{\infty}(-1)^n L_n\left(\frac{2k_\perp^2}{|b|}\right)\left[\frac{a+2n|b|}{(a+2n|b|)^2+c^2}\mathcal{P}_- \right. \\ &\left. + \frac{a+2(n+1)|b|}{[a+2(n+1)|b|]^2+c^2}\mathcal{P}_+\right], \end{aligned} \tag{D.6}$$

$$\begin{aligned} I_2 &= 2e^{-\frac{k_\perp^2}{|b|}}\sum_{n=0}^{\infty}(-1)^n L_n\left(\frac{2k_\perp^2}{|b|}\right)\left[\frac{1}{(a+2n|b|)^2+c^2}\mathcal{P}_- \right. \\ &\left. + \frac{1}{[a+2(n+1)|b|]^2+c^2}\mathcal{P}_+\right], \end{aligned} \tag{D.7}$$

$$I_3 = 4e^{-\frac{k_\perp^2}{|b|}}\sum_{n=0}^{\infty}(-1)^n L_n^1\left(\frac{2k_\perp^2}{|b|}\right)\frac{1}{[a+2(n+1)|b|]^2+c^2}. \tag{D.8}$$

Here we used the following notation:

$$a = (\omega_E + i\delta\mu)^2 + (k^3)^2 + m^2 + \Delta^2 - \bar{\mu}^2, \tag{D.9}$$

$$b = \tilde{e}\tilde{Q}\tilde{B}, \tag{D.10}$$

$$c = 2\bar{\mu}\sqrt{(\omega_E + i\delta\mu)^2 + \Delta^2}. \tag{D.11}$$

It is appropriate to mention that the use of the proper-time representations, as given by Eqs. (D.2) and (D.3), may not be completely justified in the presence of a nonzero density. Indeed, when the chemical potential is sufficiently large, the above expression for the parameter a may become negative. When this occurs, the proper-time integrals become divergent and the validity of the derivation seemingly fails. The way around this problem is to assume that the chemical potential is sufficiently small at all intermediate stages of derivation. In the end, after magnetic field expansion is done and all proper-time integrations are performed, one can extend the validity of the propagators to large values of the chemical potential.

With the above remark kept in mind, we use the proper-time representations to rewrite the expressions for the sums I_i as follows:

$$I_1 = 2e^{-k_\perp^2/|b|}\sum_{n=0}^{\infty}(-1)^n L_n\left(\frac{2k_\perp^2}{|b|}\right)\int_0^\infty ds\cos(sc)e^{-s(a+2n|b|)}\left(\mathcal{P}_- + e^{-2|b|s}\mathcal{P}_+\right), \tag{D.12}$$

$$I_2 = 2e^{-k_\perp^2/|b|}\sum_{n=0}^{\infty}(-1)^n L_n\left(\frac{2k_\perp^2}{|b|}\right)\int_0^\infty \frac{ds}{c}\sin(sc)e^{-s(a+2n|b|)}\left(\mathcal{P}_- + e^{-2|b|s}\mathcal{P}_+\right), \tag{D.13}$$

$$I_3 = 4e^{-k_\perp^2/|b|}\sum_{n=0}^{\infty}(-1)^n L_n^1\left(\frac{2k_\perp^2}{|b|}\right)\int_0^\infty \frac{ds}{c}\sin(sc)e^{-s(a+2n|b|+2|b|)}. \tag{D.14}$$

Then, after using the summation formula (D.4), we derive

$$I_1 = \int_0^\infty ds\cos(sc)e^{-sa-(k_\perp^2/b)\tanh(sb)}\left[1 - i\gamma^1\gamma^2\tanh(sb)\right], \tag{D.15}$$

$$I_2 = \int_0^\infty \frac{ds}{c}\sin(sc)e^{-sa-(k_\perp^2/b)\tanh(sb)}\left[1 - i\gamma^1\gamma^2\tanh(sb)\right], \tag{D.16}$$

$$I_3 = \int_0^\infty \frac{ds}{c}\sin(sc)e^{-sa-(k_\perp^2/b)\tanh(sb)}\frac{1}{\cosh^2(sb)}. \tag{D.17}$$

Finally, expanding the integrands in powers of the magnetic field b and integrating over the proper time, we obtain

$$\begin{aligned} I_1 \simeq & \int_0^\infty ds\cos(sc)e^{-s(a+k_\perp^2)}\left(1 - i\gamma^1\gamma^2 sb + \frac{s^3}{3}k_\perp^2 b^2 + O(b^3)\right) = \frac{a+k_\perp^2}{(a+k_\perp^2)^2+c^2} \\ & -i\gamma^1\gamma^2\frac{(a+k_\perp^2)^2-c^2}{[(a+k_\perp^2)^2+c^2]^2}b + \frac{2[(a+k_\perp^2)^4 - 6(a+k_\perp^2)^2c^2 + c^4]k_\perp^2}{[(a+k_\perp^2)^2+c^2]^4}b^2 + O(b^3), \end{aligned} \tag{D.18}$$

$$\begin{aligned} I_2 \simeq & \int_0^\infty \frac{ds}{c}\sin(sc)e^{-s(a+k_\perp^2)}\left(1 - i\gamma^1\gamma^2 sb + \frac{s^3}{3}k_\perp^2 b^2 + O(b^3)\right) = \frac{1}{(a+k_\perp^2)^2+c^2} \\ & -i\gamma^1\gamma^2\frac{2(a+k_\perp^2)}{[(a+k_\perp^2)^2+c^2]^2}b + \frac{8(a+k_\perp^2)[(a+k_\perp^2)^2-c^2]k_\perp^2}{[(a+k_\perp^2)^2+c^2]^4}b^2 + O(b^3), \end{aligned} \tag{D.19}$$

$$\begin{aligned} I_3 \simeq & \int_0^\infty \frac{ds}{c}\sin(sc)e^{-s(a+k_\perp^2)}\left(1 - s^2b^2 + \frac{s^3}{3}k_\perp^2 b^2 + O(b^3)\right) = \frac{1}{(a+k_\perp^2)^2+c^2} \\ & -\frac{2[3(a+k_\perp^2)^2-c^2]}{[(a+k_\perp^2)^2+c^2]^3}b^2 + \frac{8(a+k_\perp^2)[(a+k_\perp^2)^2-c^2]k_\perp^2}{[(a+k_\perp^2)^2+c^2]^4}b^2 + O(b^3). \end{aligned} \tag{D.20}$$

Now, combining the same-order terms in powers of the magnetic field, we rewrite

propagator (D.5) as follows:

$$\bar{S}^X_{(+\frac{1}{2})21}(i\omega_E, k^3, \boldsymbol{k}_\perp) = i\gamma^5\Delta\left[K^{(0)} + K^{(1)} + K^{(2)}\right], \tag{D.21}$$

where

$$K^{(0)} = \frac{a_k^+ + a_k^- + 4\bar{\mu}(\boldsymbol{\gamma}\cdot\boldsymbol{k} + m)\gamma^0}{2a_k^+ a_k^-}, \tag{D.22}$$

$$K^{(1)} = -i\gamma^1\gamma^2\frac{(a_k^+)^2 + (a_k^-)^2 - 4\bar{\mu}^2(a_k^+ + a_k^-) + 8\bar{\mu}a_k(k^3\gamma^3 + m)\gamma^0}{2(a_k^+ a_k^-)^2}b, \tag{D.23}$$

$$\begin{aligned} K^{(2)} = {} & \frac{a_k^+(a_k^+ - 4\bar{\mu}^2)^3 + a_k^-(a_k^- - 4\bar{\mu}^2)^3 + 4\bar{\mu}^2 a_k^+ a_k^-\left[16\bar{\mu}^2 - 3(a_k^+ + a_k^-)\right]}{(a_k^+ a_k^-)^4}k_\perp^2 b^2 \\ & -4\bar{\mu}(\boldsymbol{\gamma}_\perp\cdot\boldsymbol{k}_\perp)\gamma^0\frac{4a_k^2 - a_k^+ a_k^-}{(a_k^+ a_k^-)^3}b^2 + 16\bar{\mu}a_k(\boldsymbol{\gamma}\cdot\boldsymbol{k} + m)\gamma^0\frac{2a_k^2 - a_k^+ a_k^-}{(a_k^+ a_k^-)^4}k_\perp^2 b^2. \end{aligned} \tag{D.24}$$

Note the shorthand notation used,

$$\boldsymbol{\gamma}\cdot\boldsymbol{k} \equiv \boldsymbol{\gamma}_\perp\cdot\boldsymbol{k}_\perp + k^3\gamma^3, \tag{D.25}$$

$$a_k^\pm \equiv (\omega_E + i\delta\mu)^2 + (E_k \pm \bar{\mu})^2 + \Delta^2, \tag{D.26}$$

$$a_k \equiv a + k_\perp^2 = (\omega_E + i\delta\mu)^2 + k^2 + m^2 + \Delta^2 - \bar{\mu}^2, \tag{D.27}$$

as well as $E_k \equiv \sqrt{k^2 + m^2}$ and $k^2 \equiv k_\perp^2 + (k^3)^2$.

APPENDIX E

GAP EQUATION IN WEAK MAGNETIC FIELD LIMIT

To leading order (i.e., the limit of vanishing magnetic field), the gap equation reads

$$\Delta^{(0)}(\omega_E) = \frac{g^2}{6}\int\frac{d\omega'_E}{2\pi}\int\frac{d^3\boldsymbol{k}'}{(2\pi)^3}\Delta^{(0)}(\omega'_E)\mathrm{tr}\left[\gamma^\mu K^{(0)}(\omega',\boldsymbol{k}')\gamma^\nu\right]D_{\mu\nu}(\omega-\omega',\boldsymbol{k}-\boldsymbol{k}'). \tag{E.1}$$

Here we assumed that the gap function is an explicit function of the energy, but not of the momentum. The result for the trace in the integrand is given by

$$\mathrm{tr}\left[\gamma^\mu K^{(0)}(\omega',\boldsymbol{k}')\gamma^\nu\right] = 2g^{\mu\nu}\frac{a^+_{k'}+a^-_{k'}}{a^+_{k'}a^-_{k'}}+\ldots, \tag{E.2}$$

where the ellipsis stands for antisymmetric terms, which do not affect the form of the gap equation. Indeed, when contracted with the gluon propagator, which is symmetric in Lorentz indices, all antisymmetric terms will vanish.

At asymptotic densities, we can also neglect all corrections due to nonzero m and $\delta\mu$. By taking into account that the main contribution to the momentum integral on the right hand side of the gap equation comes from the vicinity of the Fermi surface ($k'\simeq k_F=\sqrt{\bar{\mu}^2-m^2}$), we can make the following approximation for the trace:

$$\mathrm{tr}\left[\gamma^\mu K^{(0)}(\omega',\boldsymbol{k}')\gamma^\nu\right]\simeq\frac{2g^{\mu\nu}}{a^-_{k'}}. \tag{E.3}$$

Note that, in the vicinity of the Fermi surface, one has

$$a^-_{k'} = (\omega'_E)^2+\xi^2_{k'}+\Delta^2\ll\bar{\mu}^2, \tag{E.4}$$

$$a^+_{k'} = 4\bar{\mu}^2+4\bar{\mu}\xi_{k'}+a^-_{k'}\simeq 4\bar{\mu}(\bar{\mu}+\xi_{k'}), \tag{E.5}$$

where $\xi_{k'}\equiv E_{k'}-\mu\simeq k'-k_F$.

The resulting equation coincides with the known form of the gap equation in the case of zero magnetic field studied in Refs. [56, 57, 58, 59, 60, 61, 62, 63, 64, 139, 140]. In our notation, the corresponding solution for the gap function reads

$$|\Delta^{(0)}|\simeq\Lambda\exp(-\frac{3\pi^2}{\sqrt{2}g}+1). \tag{E.6}$$

In order to find the correction to the gap function due to nonzero magnetic field, let us include the approximate kernel up to second order in the magnetic field. After taking traces on the both sides of the equation, we obtain

$$\begin{aligned}\Delta^{(B)}(\omega_E) &= \frac{g^2}{6}\int\frac{d\omega'_E}{2\pi}\int\frac{d^3\boldsymbol{k}'}{(2\pi)^3}\Delta^{(B)}(\omega'_E)\mathrm{tr}\big[\gamma^\mu K^{(0)}(\omega',\boldsymbol{k}')\gamma^\nu\big]\\ &\quad\times D_{\mu\nu}(\omega-\omega',\boldsymbol{k}-\boldsymbol{k}')+\frac{g^2}{6}\int\frac{d\omega'_E}{2\pi}\int\frac{d^3\boldsymbol{k}'}{(2\pi)^3}\Delta^{(B)}(\omega'_E)\\ &\quad\times\mathrm{tr}\big[\gamma^\mu K^{(2)}(\omega',\boldsymbol{k}')\gamma^\nu\big]D_{\mu\nu}(\omega-\omega',\boldsymbol{k}-\boldsymbol{k}'). \qquad \text{(E.7)}\end{aligned}$$

In addition to the result in Eq. (E.2), this equation also contains the trace of the second-order correction to the kernel. The corresponding approximate expression in the vicinity of the Fermi surface reads

$$\mathrm{tr}\left[\gamma^\mu K^{(2)}(\omega',\boldsymbol{k}')\gamma^\nu\right]\simeq g^{\mu\nu}\frac{N_{k'}(k'_\perp)^2}{2\bar{\mu}^4(a^-_{k'})^4}(\tilde{e}\tilde{Q}\tilde{B})^2+\ldots, \qquad \text{(E.8)}$$

where $N_{k'}\simeq 4\bar{\mu}\xi_{k'}(2\xi^2_{k'}-a^-_{k'})-24\xi^4_{k'}+16a^-_{k'}\xi^2_{k'}-(a^-_{k'})^2$ and the ellipsis denotes antisymmetric terms. Let us point that the only directional dependence of this trace comes through the overall factor $(k'_\perp)^2\equiv(k')^2(1-\cos^2\theta_{Bk'})$, where $\theta_{Bk'}$ denotes the angle between the direction of the magnetic $\boldsymbol{B}$ and the momentum $\boldsymbol{k}'$. (Strictly speaking, in a self-consistent analysis, the gap function on the right hand side will also have a directional dependence and will affect the angular integration. The corresponding effects are expected to be very small and will be neglected in the simplified analysis here.) The integrand on the right hand side of Eq. (E.7) has an additional directional dependence in the gluon propagator, see Eq. (2.34), which is a function of the polar angle $\theta\equiv\theta_{kk'}$ (i.e., the polar angular coordinate of vector $\boldsymbol{k}'$ measured from the direction of the external vector $\boldsymbol{k}$). With this convention for angular coordinates, it is convenient to use the following relation:

$$\cos\theta_{Bk'}=\sin\theta\,\sin\theta_{Bk}\,\cos(\phi-\phi_{Bk})+\cos\theta\,\cos\theta_{Bk}, \qquad \text{(E.9)}$$

in order to rewrite the expression for $(k'_\perp)^2$ in terms of the angular integration variables θ (polar angle) and ϕ (azimuthal angle). Now we can easily perform the angular integration on the right-hand side of the gap equation. The results for the two types of angular integrations, namely with the electric and magnetic part of the gluon propagator, read

$$\begin{aligned} A_{el} &= \int \frac{(1-\cos^2\theta_{Bk'})\sin\theta\, d\theta d\phi}{M^2-2k'k\cos\theta} = \frac{\pi}{8(k')^3k^3}\Bigg[2k'kM^2\left[1+3\cos(2\theta_{Bk})\right] \\ &\quad +\frac{1}{2}\Big(4(k')^2k^2\left[3+\cos(2\theta_{Bk})\right]-M^4\left[1+3\cos(2\theta_{Bk})\right]\Big)\ln\frac{M^2+2k'k}{M^2-2k'k}\Bigg], \end{aligned} \tag{E.10}$$

$$\begin{aligned} A_{mag} &= \int(1-\cos^2\theta_{Bk'})\sin\theta\, d\theta d\phi\frac{2\left[(k')^2+k^2-2k'k\cos\theta\right]^{1/2}}{\left[(k')^2+k^2-2k'k\cos\theta\right]^{3/2}+\omega_l^3} \\ &= \frac{2\pi}{3k'k}\left[1+\cos^2\theta_{Bk}+\left(\frac{(k')^2+k^2}{2k'k}\right)^2\left(1-3\cos^2\theta_{Bk}\right)\right]\ln\frac{(k'+k)^3+\omega_l^3}{|k'-k|^3+\omega_l^3} \\ &\quad +\frac{\pi\omega_l^2}{2(k'k)^3}\left(1-3\cos^2\theta_{Bk}\right)\Bigg[\omega_l^2\int_{x_{min}}^{x_{max}}\frac{x^6dx}{x^3+1} \\ &\quad -2\left[(k')^2+k^2\right]\int_{x_{min}}^{x_{max}}\frac{x^4dx}{x^3+1}\Bigg], \end{aligned} \tag{E.11}$$

where $M^2=(\omega'_E-\omega_E)^2+(k')^2+k^2+m_D^2$. In order to simplify the calculation of A_{mag}, it is convenient to change the integration variable θ to the new dimensionless variable $x=(1/\omega_l)\sqrt{(k')^2+k^2-2k'k\cos\theta}$. Note that $\sin\theta d\theta=\omega_l^2xdx/(k'k)$ and the new range of integration is from $x_{min}=|k'-k|/\omega_l$ to $x_{max}=(k'+k)/\omega_l$.

In the vicinity of the Fermi surface, the approximate results for this integrals read

$$A_{el} \simeq \frac{\pi\sin^2\theta_{Bk}}{\bar{\mu}^2}\ln\frac{(2\bar{\mu})^2}{(\omega'_E-\omega_E)^2+(k'-k)^2+m_D^2}+\ldots, \tag{E.12}$$

$$A_{mag} \simeq \frac{4\pi\sin^2\theta_{Bk}}{3\bar{\mu}^2}\ln\frac{(2\bar{\mu})^3}{|k'-k|^3+\omega_l^3}+\ldots, \tag{E.13}$$

where the ellipses denote the subleading terms.

By making use of the above intermediate results, we arrive at the following form of the gap equation,

$$\Delta^{(B)}(\omega_E) = \frac{2g^2}{9}\int_{-\infty}^{\infty}\frac{d\omega'_E}{(2\pi)}\int\frac{d\xi_{k'}}{(2\pi)^2}\frac{\Delta^{(B)}(\omega'_E)}{a^-_{k'}}\ln\frac{(2\bar{\mu})^3}{|k'-k|^3+\omega_l^3} \times\left(1+\frac{\left[-24\xi^4_{k'}+16a^-_{k'}\xi^2_{k'}-(a^-_{k'})^2\right](\tilde{e}\tilde{Q}\tilde{B})^2}{(2\bar{\mu})^2(a^-_{k'})^3}\sin^2\theta_{Bk}\right). \quad \text{(E.14)}$$

Recall that $\omega_l^3=(\pi/4)m_D^2|\omega'_E-\omega_E|$. Integrating over the momentum, we arrive at

$$\Delta^{(B)}(\omega_E) = \frac{g^2}{36\pi^2}\int_{-\infty}^{\infty}d\omega'_E\Delta^{(B)}(\omega'_E)\left[\frac{1}{\sqrt{(\omega'_E)^2+(\Delta^{(B)})^2}}\ln\frac{\Lambda}{|\omega'_E-\omega_E|} +\frac{9\omega_l^{15}(\tilde{e}\tilde{Q}\tilde{B})^2\sin^2\theta_{Bk}}{4\bar{\mu}^2\left(\omega_l^6+[(\omega'_E)^2+(\Delta^{(B)})^2]^3\right)^3}\ln\frac{\omega_l}{|\omega'_E-\omega_E|}\right]. \quad \text{(E.15)}$$

To get a rough estimate, let us take an infrared cutoff in the energy integration at $\omega'_{IR}\simeq\Delta^{(B)}$ and drop the dependence on $\Delta^{(B)}$ in the denominator of the integrand. Then, we have

$$\Delta^{(B)} \simeq \frac{g^2}{18\pi^2}\int_{\Delta^{(B)}}^{\Lambda}d\omega'_E\frac{\Delta^{(B)}}{|\omega'_E|}\left(1+\frac{54(\tilde{e}\tilde{Q}\tilde{B})^2\sin^2\theta_{Bk}}{\pi\bar{\mu}^2m_D^2}\right)\ln\frac{\Lambda}{|\omega'_E|}. \quad \text{(E.16)}$$

This means that the magnetic field correction is equivalent to an effective increase of the coupling constant, i.e.,

$$g^2\to g^2_{eff}=g^2\left(1+\frac{54\pi(\tilde{e}\tilde{Q}\tilde{B})^2}{g^2\bar{\mu}^4}\sin^2\theta_{Bk}\right), \quad \text{(E.17)}$$

where we used the definition of the Debye mass $m_D^2=(g\bar{\mu}/\pi)^2$.